1992

# Sediment transport of fine-grained alluvium from Cooper Creek, Central Australia

Jerry Christopher Maroulis
*University of Wollongong*

# SEDIMENT TRANSPORT OF FINE-GRAINED ALLUVIUM FROM COOPER CREEK, CENTRAL AUSTRALIA

JERRY CHRISTOPHER MAROULIS



Thesis submitted in partial fulfilment of the requirements
for the Honours Degree of Master of Science
in the Department of Geography
The University of Wollongong
May 1992

**Except where acknowledged in the text, this thesis is my own work and does not contain material previously published or written by any other person, nor has it been submitted for a higher degree at any other university.**

## DEDICATION

Brian Rust
In memoriam

If I have seen further
it is by standing
on the shoulders of giants.

- Sir Isaac Newton

## ABSTRACT

The ability of mud aggregates to form depositional bedforms is of considerable sedimentological importance for explaining the geomorphology of the Channel Country of Central Australia as well as the depositional environment of certain argillaceous fluvial sequences in the rock record. The sediment transport and bedform development of an aggregated sediment obtained from the floodplain of Cooper Creek, Central Australia, was examined in a laboratory flume over a range of flow conditions. The aggregates were found to be clay-rich (>60% clay), fine sand-sized ($d_{50}$=0.10 mm), low density (2300 kg.m$^{-3}$), water-stable and contained very low salt levels (<0.02%). The presence of smectite in the clay mineralogy of the sediment is an important factor in the development of the aggregates. Disaggregated sediment could be reaggregated in a laboratory after 2-3 wetting/drying cycles under simulated field conditions. Bedforms of aggregated mud ranging from lower-regime plane beds to upper-regime antidunes were observed. In the flume, the aggregates moved predominantly as bedload with measured peak bedload concentrations being high compared to other flume studies. The highly mobile nature of the sediment is due to the ready entrainment of low-density aggregates. The occurrence of braid bars formed of mud in an extensive low-gradient arid environment evident in the Channel Country of Central Australia, can be attributed to steeper braid-channel gradients across the floodplains during the passage of a flood; the highly mobile nature of the low-density sediment aggregates; the ability of the aggregates to be transported as bedload and their durable nature within the flow.

## ACKNOWLEDGMENTS

In the course of writing this thesis there have been many people who have assisted me. I will attempt here to thank all those responsible.

Firstly I am greatly indebted to my supervisor Associate Professor Gerald Nanson whose drive, vitality and enthusiasm inspired me to see this thesis to fruition. Thanks must also go to my good friend Dr. Richard (Bert) Roberts who assisted me in the field and for his many words of wisdom. Many thanks to Hilda Shaw for being so supportive and helpful, to Richard Miller for his assistance in preparing diagrams, and to all the staff in the Department of Geography at the University of Wollongong that made me feel at home whenever I ventured southwards to work on the thesis.

I must also thank my family (Mum, Dad, Maria, Nick, Jimmy and Johnathon) for their patience in putting up with me for so long, especially during my unpredictable moods. I love you all very much. To my adopted family the Sherratt's in Toowoomba, thank you for your time and moral support, especially my *mate*, Anthony who has been a tower of strength when times got tough. Also thanks go to Tina Baartz and family for being good listeners and to the Young family for providing me access to computing facilities. To my very dear friend Dianne Atkins, thanks for being a true friend and for being there whenever I needed encouragement.

To my many dear friends (R. Loch, M. Silburn, R. Connolly, C. Ciesiolka, J. Foley, G. Wockner and K. Myers) in the Land Management

Research Branch of the Queensland Department of Primary Industries in Toowoomba thanks for all your assistance. Also I must thank all my friends and colleagues at Glennie Memorial School in Toowoomba for allowing me access to their computer facilities and for their encouragement and moral support.

Finally, thanks go to my very dear friend in Brisbane, Vickie Williams who has made such a lasting impression in my life. For being so loving, caring, supportive, and for inspiring me to complete this thesis, I am greatly in your debt.

## CONTENTS

## LIST OF FIGURES

## LIST OF PLATES

## LIST OF TABLES

# CHAPTER 1 INTRODUCTION

Cooper Creek is one of several extensive low-gradient rivers that form the Channel Country in the north-eastern part of the Lake Eyre Basin of Central Australia. These rivers transport primarily clay-rich mud through a complex mosaic of two coexistent channel planforms; braided and anastomosing (Nanson et al., 1986). They attributed the previously unrecognised occurrence of braided channels formed of mud to the transport of clay-rich sediment as fine sand-sized pedogenic aggregates with a density lower than that of quartz grains (Nanson et al., 1988). The ability of the aggregates to form alluvial bedforms is a phenomenon that required further investigation, for it has important implications for understanding the sedimentary stratigraphy in the rock record (Rust and Nanson, 1989) as well as contemporary processes that control sediment transport and erosion in these extensive areas of inland Australia (Nanson et al., 1988).

This study has two broad aims: firstly, to assess the pedogenic mechanisms associated with the formation of the disaggregated mud into sand-sized aggregates available for fluvial transport as bedload in Cooper Creek; and secondly, to examine in a laboratory flume the transport characteristics and bedform development of these mud-aggregates.

The flume experiments examine the sediment transport and hydrodynamic properties of aggregated muddy sediment and show the aggregates to be extremely water-stable and to produce bedforms ranging from lower-regime plane beds and ripples through to upper-regime plane beds and antidunes. There is agreement, but also interesting differences, between published bedform existence diagrams for quartz sand and the experimental results presented here for sand-sized aggregated mud pellets.

This study provides a greater understanding of the pedogenic processes leading to the formation of aggregated mud pellets in an alluvial environment and helps to explain sediment transport in low-gradient, mud-load systems such as Cooper Creek in western Queensland. Of relevance to sedimentologists is an understanding of the transport and depositional conditions leading to the preservation of analogous argillaceous fluvial sediments in the rock record.

Sediment for this investigation was collected from the floodplain of Cooper Creek between Durham Downs and Naccowlah (Figure 1.1) where extensive work has been done on the sedimentary and stratigraphic character and chronology of the river system (Nanson et al., 1986; Rust and Nanson, 1986; Nanson et al., 1988).

## 1.1 <u>Physiography of Cooper Creek.</u>

Cooper Creek is the largest of three major river systems draining the Channel Country of the Lake Eyre Basin. These are the Diamantina and Georgina Rivers which, collectively with Cooper Creek, drain an area of approximately 700 000 km$^2$ of arid Central Australia (Figure 1.1).

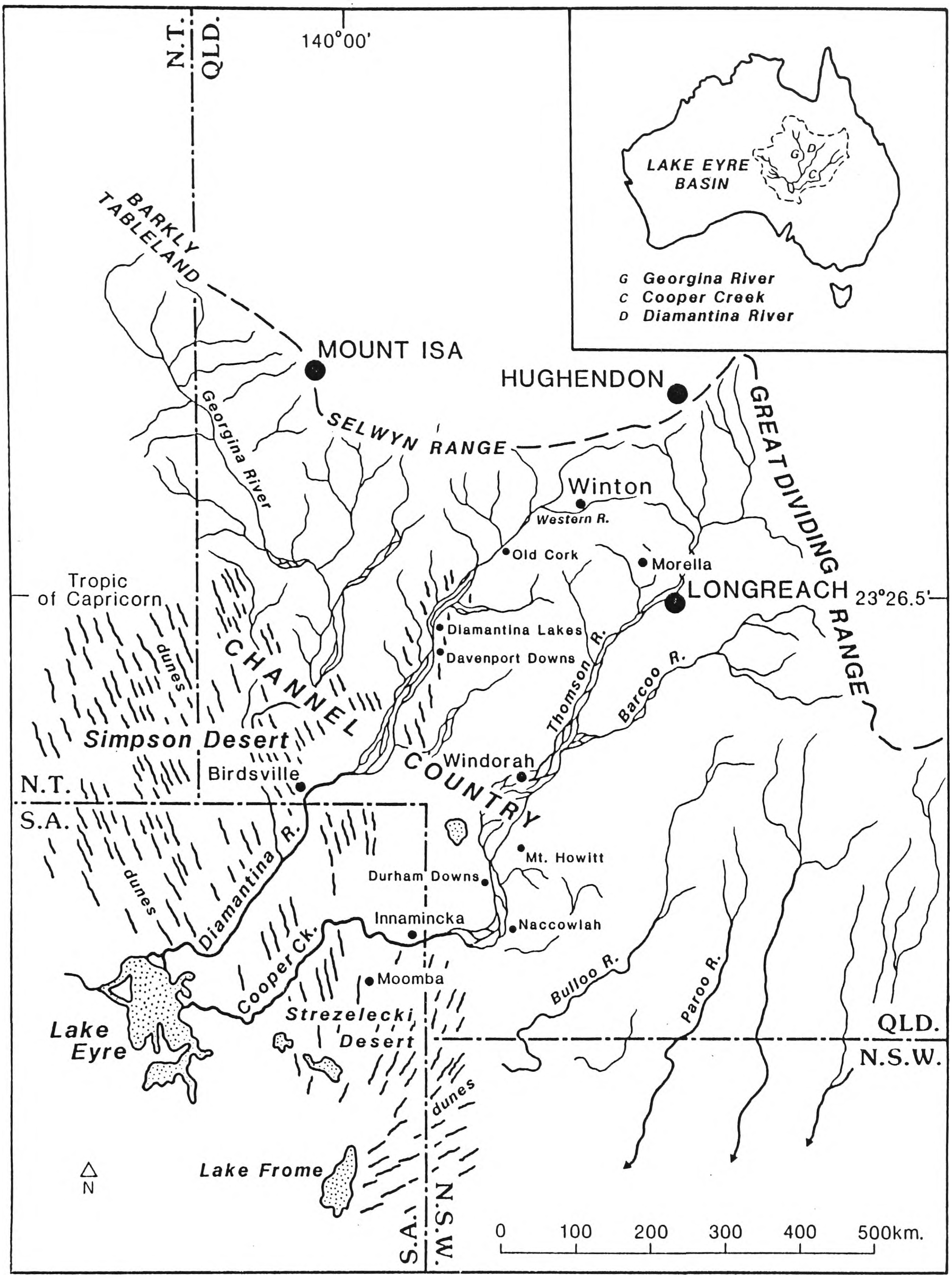


Figure 1.1 The northeastern part of the Eyre Basin showing the location of the study site at Naccowlah on Cooper Creek.

These rivers are characterised by very low channel gradients (<0.0002 m/m) and a vast and complex array of fluvial landforms including narrow anastomosing channels and wide shallow braid channels separated by broad braid bars. In general, channel patterns are braided over the surface of very extensive floodplains formed of mud. Aerial photographs of the Cooper floodplain south of Durham Downs illustrate both channel types (Plates 1.1-1.3).

## 1.2 Hydrology

Rainfall in the Lake Eyre Basin ranges from 400-500 mm/year in the headwaters of the Cooper to less than 100 mm/year in the Simpson Desert (Figure 1.2). Flooding in the basin is extremely erratic (Nimmo, 1974). Consequently Lake Eyre fills only several times each century (Nanson et al., 1988). Discharges in the Cooper decrease markedly downstream due mainly to seepage and evaporation that exists in the maze of distributary channels, ephemeral lakes, clay pans, aeolian dunes and floodbasins between Windorah and Lake Eyre (Plates 1.1-1.3).

## 1.3 Geology

The Great Artesian Basin is intracratonic and bordered by strong positive structures (Twidale, 1972). It is a basin of internal drainage and has long been a depository for sediments. In the early Cretaceous there was a

Plate 1.1 Oblique aerial view of Cooper Creek showing sinuous anastomosing anabranches and the braided floodplain surface looking north towards Durham Downs.

Plate 1.2 Oblique aerial view of the Cooper floodplain showing a series of mud braids and some low sinuosity anabranching channels of the anastomosing system.

Plate 1.3 Oblique aerial view looking south from Naccowlah of a remnant aeolian sand dune. Overbank deposition in this backswamp of the Cooper floodplain is slowly burying the sand dune.

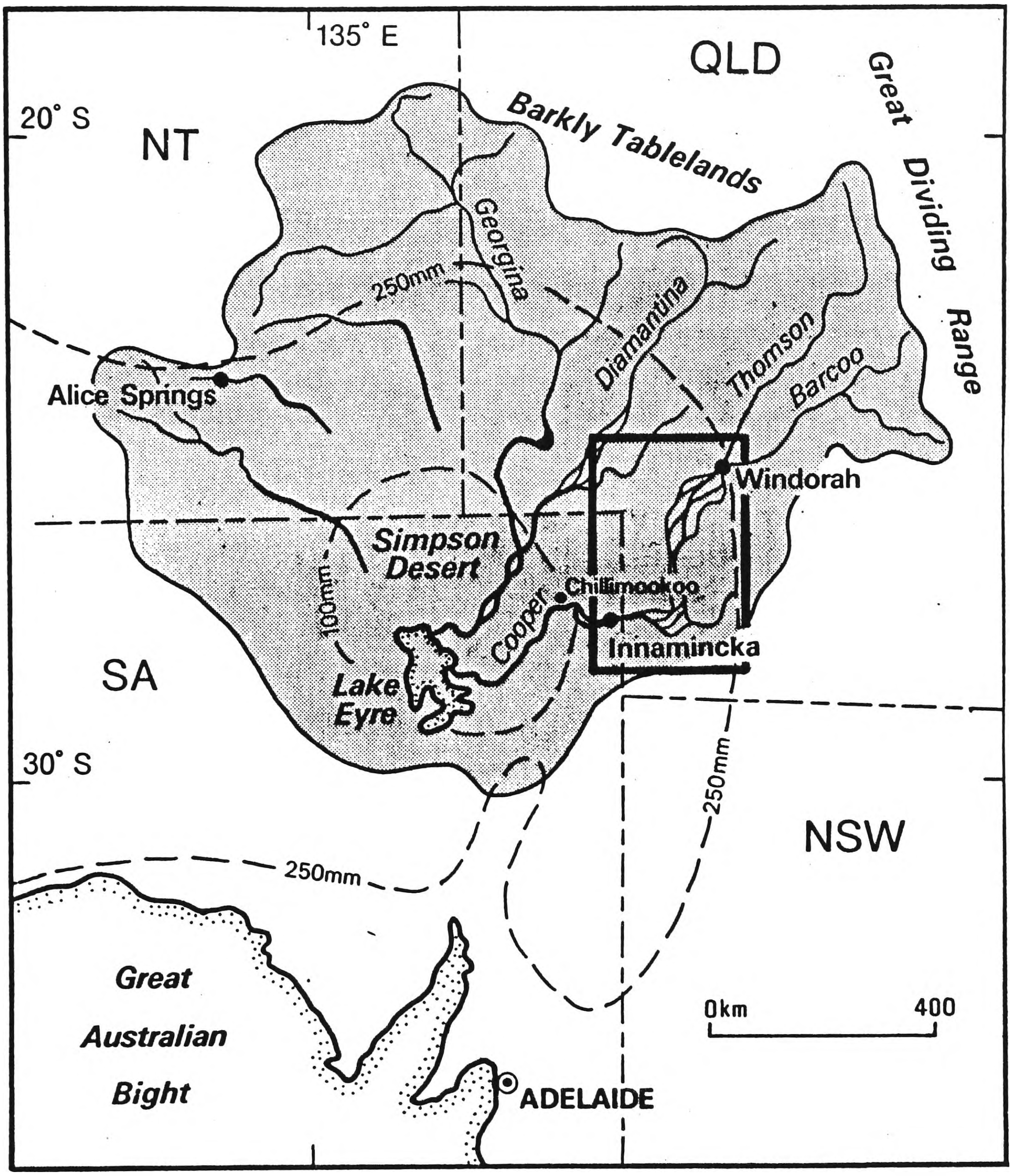


Figure 1.2 Location of study area and isohytes of mean annual rainfall within Lake Eyre Basin (dashed lines). Represented channel patterns on Cooper Creek are highly generalized.

prolonged marine transgression. During the Cainozoic, lacustrine and fluviatile deposition alternated with weathering and erosion over much of the region. There has been little tectonic activity in this area since the mid-Mesozoic (Dawson, 1974).

Thick Quaternary alluvium covers extensive areas of the Channel Country. At Lake Yamma Yamma, a tributary lake fed by the Cooper 100 km north of Durham Downs, over 100 m of alluvia has been recorded (Dawson, 1974) displaying alternating bands of sand and mud.

Dune and sheet sand cover large areas to the south and west of Cooper Creek. In places this predominantly red, quartzose sand covers Quaternary alluvium and in other areas the Tertiary landscape. Much of the Quaternary sand in this area is believed to be reworked, late Tertiary, fluviatile deposits (Whitehouse, 1947; Dawson, 1974) although there is no direct evidence of this.

## 1.4 Vegetation

Vegetation on the Cooper floodplain is predominantly comprised of bluebush (Chenopodium auricomum), lignum (Muelhenbeckia cunninghamii), river red gum (E. camaldulensis) and coolibah (E. microtheca) with cooper clover (Trigonella suavissama) and/or channel millet (Echinochloa turnerana) dominating the ground flora after floods. Coolibah open woodland is associated with waterholes and billabongs (Boyland, 1974).

## 1.5 <u>Soils</u>

Grey clays (Stace et al., 1968; Northcote, 1965) are the predominant soil type on the Cooper floodplain and consist of dark, self-mulching, very deep, heavy grey clays with deep wide cracks when dry and sometimes exhibiting gilgai patterning (Dawson and Ahern, 1974). With a clay content typically greater than 50% they are commonly known as Vertisols and contain smectite (an expandable clay) which enables the soil to swell and shrink. Nanson et al. (1988) maintain that rain or flooding, followed by intense baking under a hot sub-tropical sun appears to be a sufficient mechanism to develop and maintain the aggregated form of the sediment (Nanson et al., 1988).

# CHAPTER 2 RESEARCH TO DATE

## 2.1 Aggregated sediment

### 2.1.1 Characteristics of the clay aggregates

Vertisols are typically composed of a high proportion of montmorillonite (smectite), however those of the Channel Country have mixed or even kaolinitic mineralogy (Rust and Nanson, 1989). The presence of smectite is thought to be responsible (Nanson et al., 1986; Nanson et al., 1988) for the repetitive swelling and shrinking of these soils.

The Cooper floodplain is characterised by clay-rich mud aggregates that exist over a vast area along the river valleys of the eastern part of the Lake Eyre Basin of Central Australia (Nanson et al., 1986; Nanson et al., 1988; Rust and Nanson, 1989). Similar aggregates have also been reported in fluvial sediments elsewhere by Williams (1970), in lacustrine sediments by Bowler (1973) and Dare-Edwards (1982) and in agricultural soils by Loch et al., (1989) and Maroulis et al. (in press). But to date there have been no detailed observations on how the aggregates form and what specific conditions are required, although Bowler (1973) has proposed a mechanism in saline lakes.

### 2.1.2 Theories on the origin of the aggregates

While various theories have been put forward, the exact origin of the aggregates has been a contentious issue in the literature. Butler (1956) and

Bowler (1973) observed the development of clay aggregates (pellets) in playa lakes of Central Australia. They suggested that the highly saline lake waters helped to aggregate fine clays washed in during flooding. Aeolian processes transport the aggregates from the dry playa lake-bed onto lunettes on the lee side and possibly further afield such as onto adjacent floodplains.

In contrast, Nanson et al. (1986, 1988) and Rust and Nanson (1989) argue that for the Cooper floodplain, salt is unimportant. Cooper Creek is a non-saline environment as halite concentrations in the waterholes and floodplain soils were in the order of 100 ppm or less, a level insufficient to be a major factor in the development of the aggregates (Nanson et al., 1986). Nanson et al. (1988) suggested that pedogenic mud aggregates are formed during the weathering processes of argillaceous rocks in the basin and the aggregates continue to form as a result of pedogenesis on the floodplain soils.

Rust (1986) argued that the aggregates could be either biogenic in origin such as with faecal pellets, or formed in situ on the floodplain by pedogenic processes. The biogenic theory is unlikely given the aridity of the environment and the vast area over which they are found (Rust and Nanson, 1989). Nanson et al. (1988) observed pelleted muds in regolith overlying weathered shales in the upper catchment and reasoned that frequent wetting and drying cycles and the presence of expanding clays in these self-mulching soils results in pelletization of the clays both in the regolith soils and on the extensive floodplains downstream.

### 2.1.3 The link between soil-erosion research and sedimentology

Soil scientists from as early as 1960 have been aware of the unique characteristics of aggregates in soils such as Vertisols. This includes their ability to self-mulch, swell and crack, reaggregate and be transported by overland flow in rills and small headwater channels as rolling bedload aggregates. There are many reports of aggregated material in sediment eroded from headwater catchments in rill-flow and drop-impacted shallow flow (Weakly, 1962; Long, 1964; Swanson and Dedrick, 1965; Gabriels and Moldenhauser, 1978; Alberts et al. 1983; Mitchell et al. 1983; Gilley et al. 1986; and Lu et al. 1988). For clay soils rich in smectite, similar to those of the Cooper floodplain, Loch and Donnollan (1983a,b) and Loch et al. (1989) reported that the majority of sediment is aggregated.

In agricultural catchments, Lovell and Rose (1988) noted that "sediment eroded by water consists largely of soil aggregates". Similarly, Aziz and Scott (1989) state that "soil eroded and transported in channels is usually made up of individual particles and aggregates".

Research in headwater catchments illustrates that soils (including cracking clay soils) are initially entrained as aggregated material, and that the aggregates are relatively stable during transport in turbulent overland flows (Loch and Donnollan, 1983a,b). Nanson et al. (1986), Rust and Nanson (1986) and Nanson et al. (1988) have shown that the aggregated sediments probably form over vast areas of the Cooper floodplain and are sufficiently stable to survive prolonged transport resulting in the formation of an extensive contemporary braided channel network tens of kilometres wide and many hundreds of kilometres in length.

The tendency for soils rich in smectite clay to "self-mulch" is widely recognised. Coughlan (1984) noted that self-mulching requires "low stability to immersion wetting, lack of dispersion, and high shrink-swell capacity", conditions that are an exact description of alluvium in the Channel Country which is rich in smectite clay with calcium being the dominant cation adsorbed to the clay. Nanson et al. (1988, 1989) state that smectite is a minor component of the floodplain soils in downstream areas, yet cracking of the dry floodplain soil at those sites gives clear evidence of shrink/swell behaviour.

The presence of aggregates in floodplain soils is not evidence that those soils were formed from transported and deposited aggregates. Dispersed clay could form aggregates *in situ* during several wetting and drying cycles. Smith (1984) found that aggregates dispersed by puddling of clay soils re-aggregated after three wetting and drying cycles, and that this was most effective for soils with abundant smectite.

There is obviously similarity between the transport of coarse aggregates in rills during runoff events on the fertile self-mulching, clay-rich black earths of the Darling Downs (Loch and Donnollan, 1983 a,b; Loch et al., 1989; Maroulis et al., in press) and that observed in the channels and on the floodplains of Cooper Creek (Nanson et al., 1986), although the scale of the transport environment on Cooper Creek is orders of magnitude larger and over very much lower gradients.

## 2.2 Bedload sediment transport

There is a vast literature on bedload transport and numerous experiments have been conducted both in the laboratory, starting with Gilbert (1914), and in the field. Whether to run field or laboratory tests is governed by the objectives and budget of an investigation. Each has its advantages and disadvantages, as detailed below in Table 2.1.

| **Characteristics of flume and field-based experiments** | |
|---|---|
| **Flumes** | **Field** |
| - limited depth and discharge but slope and velocity can be varied. | - greater depths and discharges but constant slope. |
| - constant width. | - width is a function of flow and bank conditions. |
| - largely 2-D flow. | - 3-D flow. |
| - ability to generate higher Froude No. than in river channels (due to steeper gradients and lower flow depths). | - energy slope is relatively constant therefore, Froude Nos. are less variable. |
| | **TABLE 2.1** |

In this study, it was most practicable to examine the transport characteristics of the aggregated sediment in a laboratory flume over a range of flow discharges, velocities, depths and slopes. Measurements over such variations would be almost impossible in the field. Furthermore, through the perspex sides of the flume it was feasible to view the development of bedforms, something not viable in the field due to the turbid nature of the flow.

Flume studies also vary in the type of sediment under investigation. Most have used sands of varying grades, from very fine through to coarse sands and gravels, but few have investigated silts and/or clays in a flume. Parthenides (1965), Graf (1971) and Mantz (1978) have studied the transport of clays in a flume but were not concerned with sediment transport and bedform development in their studies. The most noteable exception being the flume study by Jopling and Forbes (1979) which used a fine silt of glacio-fluvial origin. However, to date there have been no detailed studies of clays transported as mud aggregates.

## 2.3 Bedform Characteristics

### 2.3.1 Nomenclature for bedforms.

There has been a great deal of confusion in the literature with the terminology used to describe bedforms. The American Society of Civil Engineers (A.S.C.E) (1966) produced a report from their Task Force on Bed Forms in Alluvial Channels which outlines the most commonly used definitions for bedforms. A Task Force (1968) discussion paper proposed that, in general, with increasing discharge there is a progression of bedforms as follows: ripples, dunes, flat bed, antidunes, and chutes-and-pools (Figure 2.1).

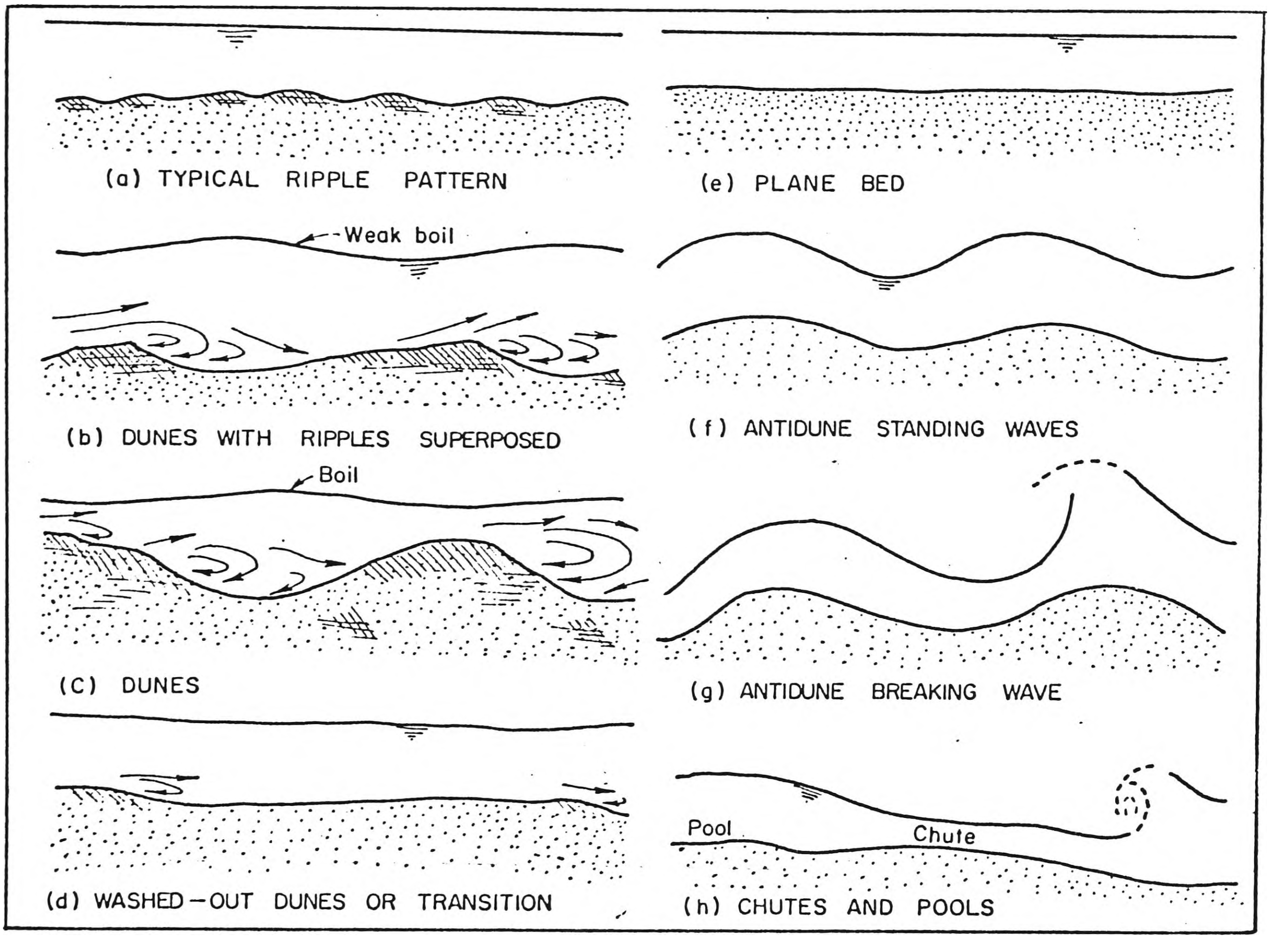


Figure 2.1 Idealized diagram of the forms of bed roughness in an alluvial channel (after Simons, et. al., 1965).

Flow in alluvial channels can be classified into an upper and lower flow-regime where the Froude number is greater and less than unity, respectively. But numerous studies have shown that the lower to upper flow regime transition takes place at Froude numbers less than one (Kennedy, 1963; Cheel, 1990). These two regions are separated by a transition zone characterised by flat-bed conditions (Simons et al., 1965). Simons et al. (1965) developed a classification of bedform structures based on flow regime (Table 2.2) which also considers the mode of sediment transport, process of energy dissipation, and phase relation between bed and water surface.

**Classification of Flow Regime (Simons et al., 1965)**

| Flow Regime | Bedform | Bed Material Concentration (ppm) | Mode of sediment transport | Type of roughness | Phase relation between bed and water surface |
|---|---|---|---|---|---|
| Lower regime | Ripples | 10-200 | Discrete steps | Form roughness predominates | Out of phase |
| | Ripples on dunes | 100-1200 | | | |
| | Dunes | 200-2000 | | | |
| Transition | Washed out dunes | 1000-3000 | | Variable | |
| Upper regime | Plane beds | 2000-6000 | Continuous | Grain roughness predominates | In phase |
| | Antidunes | >2000 | | | |
| | Chutes and Pools | >2000 | | | |

**TABLE 2.2**

One of the most contentious issues evident in the literature is the distinction between ripples and dunes. Numerous terms exist to represent these bedforms. For instance, ripples can be labelled small ripples (Simons et al., 1965; Simons and Richardson, 1966; Guy et al., 1966; Rees, 1966; Allen, 1968; Jopling and Forbes, 1979; Reineck and Singh, 1980), small-scale ripples (Allen, 1968), erosive ripples (Mantz, 1978), current ripples (Allen, 1985b) or minute ripples (Stanley, 1974). Dunes (Simons et al., 1965; Simons and Richardson, 1966; Guy et al., 1966; Engelund, 1966; Southard, 1975; Middleton and Southard, 1978; Richards, 1980; Ashley, 1990; Boguchwal and Southard, 1990; Southard and Boguchwal, 1990) are often known as megaripples (Dalrymple et al., 1978; Reineck and Singh, 1980), sand waves (Southard, 1975; Middleton and Southard, 1978), or even large ripples (Rathbun and Guy, 1967; Middleton and Southard, 1977; Harms et al., 1975, 1982) and large-scale ripples (Allen, 1968).

No attempt will be made here to debate the ripple/dune classification. Instead this study will adopt the classification scheme outlined by Ashley (1990) to distinguish dunes from ripples. Ashley (1990) summarises the findings of the 1987 SEPM (Society for Sedimentary Geology) Symposium entitled "Classification of Large-Scale Flow-Transverse Bedforms" with the aim of standardizing the multiplicity of terms used to label bedform structures. This classification represents a morphologically-based system with an underlying genetic rationale (Ashley, 1990), which is presented in Table 2.3. The size characteristics given for ripple and dune bedforms were derived from research on sand-sized sediment which could be inappropriate for this study but the relative scale differences may be relevant.

### 2.3.2 Bedform development in fine alluvium.

The development of bedforms in quartz sand is widely reported in the literature (e.g., Gilbert, 1914; Simons et al., 1965; Engelund, 1966; Guy et al. 1966, Simons and Richardson, 1966; Rathbun and Guy, 1967; Dalrymple et al., 1978; Reineck and Singh, 1980; Allen, 1968; 1985a; Ashley, 1990) but very little has been reported on the development of sedimentary structures in sediment dominated by silts and clays.

Simons et al. (1965) realised the importance of this and noted that " ... sedimentary structures formed in streams with cohesive beds or banks .. have not been subjected to intensive laboratory studies .. the development of traditional sedimentary structures in streams with cohesive beds presents an important area for future research." (p.45). Southard (1971) states that "Unfortunately, there have been no observations on bed configurations in sands or silts finer than 0.08 mm in flumes long enough for dunes to be evident if stable." (p.43).

Since then studies of fine silt have been undertaken by Rees (1966), Southard and Harms (1972), Mantz (1978) and Jopling and Forbes (1979). Sedimentary structures observed includes plane bed (no motion), small ripples for lower regime flow and a plane bed (with sediment motion) for upper regime flows. Mantz (1978) revealed some incipient dune development in fine silts while Jopling and Forbes (1979) reported antidunes at higher flow regimes. To date, only Nanson et al. (1986) has shown that a range of primary sedimentary structures can be generated in a flume using a clay-rich aggregated sediment.

| Nomenclature for Primary Sedimentary Structures. | |
|---|---|
| **Bedform** | **Description and Source of Information** |
| **- Plane Bed (no sediment motion)** | - an alluvial bed devoid of bedforms (A.S.C.E., 1966; Reineck and Singh, 1980). |
| **- Ripples** | - small bedforms whose scale is independent of depth but influenced by bed material size (Jopling and Forbes, 1979),<br>- small bedforms with wavelengths of < 30 cms and amplitudes of between 0.3-3 cms (A.S.C.E., 1966; Simons et al., 1965; Simons and Richardson, 1966),<br>- steep downstream slopes and gentle upstream slopes (Reineck and Singh, 1980). |
| **- Dunes** | **-First Order Descriptors:** *Height, $H=0.0677L^{0.8098}$ (Fleming, 1988) |
| | **Small / Medium / Large / Very Large**<br>**Size:** Spacing (m) 0.6-5 / 5-10 / 10-100 / >100<br>Height*(m): 0.075-0.4 / 0.4-0.75 / 0.75-5 / >5<br>**Shape:** 2-Dimensional<br>3-Dimensional |
| | **-Second Order Descriptors:** |
| | - Superposition: simple or compound (sizes and relative orientation)<br>- Sediment characteristics (size, sorting) |
| | **-Third Order Descriptors:** |
| | - Bedform profile (stoss and lee slope lengths and angles)<br>- Fullbeddedness (fraction of bed covered by bedforms)<br>- Flow structure (time-velocity characteristics)<br>- Relative strengths of opposing flows<br>- Dune behaviour-migration history (vertical and horizontal accretion) (Ashley, 1990). |
| **- Plane Bed (with sediment motion)** | - little vertical relief in bedforms larger than the maximum size of the bed material (A.S.C.E., 1966; Reineck and Singh, 1980). |
| **- Antidunes** | - bedforms that are in phase and interact with gravity water-surface waves; can move upstream, downstream or remain stationary (A.S.C.E., 1966),<br>- build up with time from a plane bed (Simons et al., 1965; Simons and Richardson, 1966). |
| **- Chutes and Pools** | - occur at large slopes and sediment discharges where large mounds of sediment form chutes on which the flow is supercritical, connected by pools in which the flow is supercritical or subcritical (A.S.C.E., 1966; Simons et al., 1965; Simons and Richardson, 1966). |
| | **TABLE 2.3** |

Numerous bedform existance diagrams have been developed over the last 30 years to represent the relationship between bedform types and flow and sediment size parameters (Simons et al., 1965; Guy et al., 1966; Allen, 1968; Southard, 1971; Middleton and Southard, 1978; Boguchwal and Southard, 1990; Southard and Boguchwal, 1990). The earliest bedform existance diagrams depicted bedforms as a function of stream power and sediment size for upper, transitional upper flow regimes (Simons et al., 1965; Guy et al., 1966; Allen, 1968). These diagrams have important geological applications for determining the stream energy of ancient channels where the median fall diameter and sedimentary structures are known (Simons et al., 1965).

Other researchers have used dimensionless analysis to illustrate equilibrium bed-phase stability fields, such as depth-velocity-sediment size (Southard,1971; Southard and Harms, 1972; Middleton and Southard, 1978). These have recently been upgraded (Boguchwal and Southard, 1990; Southard and Boguchwal, 1990) so that flow depth and flow velocity are used to characterize the flow.

Figure 2.2 presents a plot of mean velocity against median sediment size (standardized to 10$^{o}$C water temperature) showing stability fields of the observed bed phases for a mean flow depth between 0.25-0.40 m (Ashley, 1990). This is one of nine graphs presented by Southard and Boguchwal (1990) [p.664-5] for variable flow depths ranging from 0.015 m to 1.0 m. Data are presented for a wide range of flow depth and velocity including sediment size as low as 0.09 mm. As in earlier diagrams (Simons et al., 1965; Guy et

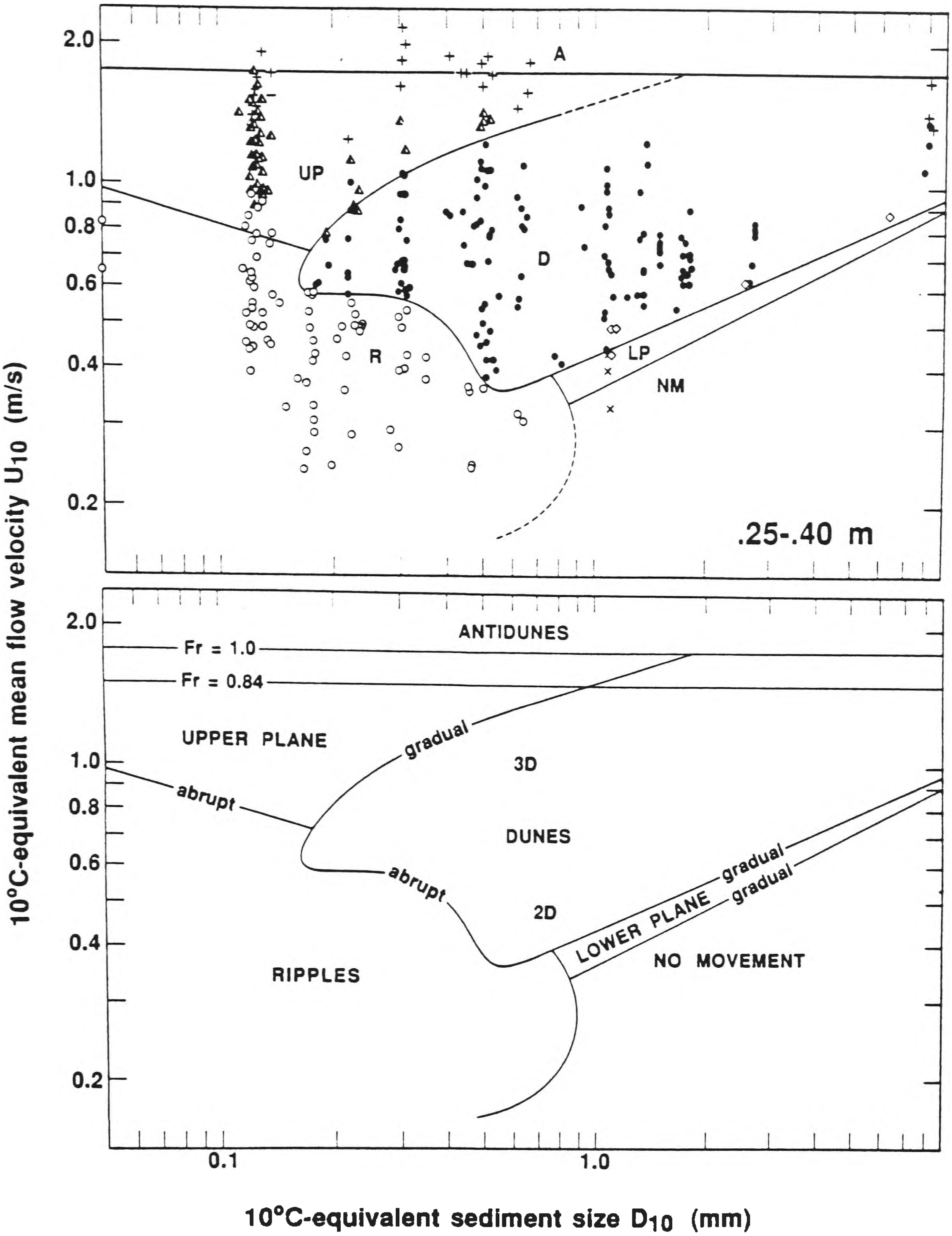


**FIGURE 2.2 (Top)** Dimensionless velocity-sediment size graph for 10°C-equivalent flow depths 0.25-0.40 m. NM=no movement; R=ripples; D=dunes; LP=lower regime plane bed; UP=upper-regime plane bed; A=antidunes.

**FIGURE 2.2 (Bottom)** Schematic version of dimensionless velocity-size graph above showing similar shape and position of the boundaries between bed phases (Modified from Southard and Boguchwal, 1990).

al., 1966; Allen, 1968) the boundary between dunes and ripples diminishes at sediment sizes less than 0.02 mm. This is substantiated by data points obtained from 39 flume studies and plotted in Figure 2.2 (Boguchwal and Southard, 1990). Based on this diagram, it appears unlikely that dunes develop in sediment of median grain size less than 0.10 mm.

The succession of bedforms (Figure 2.1) is determined partly by the size of the sediment being transported. For instance, Bagnold (1956) found that ripples do not exist in quartz sands of median diameter greater than about 0.67 to 0.71 mm whereas Simons et al. (1965) found a mean diameter of 0.6 mm was the upper limit for the existence of ripples. Recent flume experiments have shown that dunes are not likely to form in sediment with a fall diameter of <0.1 mm (Reineck and Singh, 1980). While this study could help extend the knowledge base for bedform structures in sediment with median diameters finer than 0.2 mm (Figure 2.2), the results would not be comparable to earlier work because the aggregated sediments studied here are of lower density than quartz grains (Nanson et al., 1986). Nevertheless, they stand as an interesting and unique data set for the transport of aggregated muds and the bedform existence diagram provides a useful contrast to those developed for quartz sand.

## 2.4 Flume study by Jopling and Forbes (1979)

Apart from this study and that by Jopling and Forbes (1979), very few have observed and reported in detail the development of depositional bedform features in sediment with median diameters of < 0.1 mm. The authors examined the transport and deposition of a non-aggregated coarse silt of glaciofluvial origin ($D_{50}$=0.045 mm) in a small recirculating flume. They reported on the flow hydraulics, depositional bedforms and bedding laminations observed. They observed ripples at lower flow regimes, and plane bed and antidune development in the upper flow regime stating that dunes were not observed.

## 2.5 Conclusion

Vertisols are clay-rich aggregated, water-stable soils which contain expandable clays (such as smectite) enabling them to self-mulch as reported in both agricultural and fluvial environments. However, little is known about how they form aggregates in non-saline conditions or on the bedload fluvial transport characteristics of these clay-rich sediments. An understanding of these would help explain the complex channel planforms which exist in the Channel Country rivers of central Australia, and provides a mechanism for the formation of barely recognised fluvial sequences in the sedimentary record.

The ability of this sediment to develop primary depositional sedimentary structures (Nanson et al., 1986) similar to those obtained for equivalent sized quartz sands, is worthy of further investigation. It has important implications for understanding certain argillaceous fluvial environments from the rock record as well as contemporary processes that control sediment transport and erosion in extensive areas of inland Australia.

# CHAPTER 3 METHODOLOGY

## 3.1 Sediment Collection

Sediment for the flume experiments was collected from the upper 10 cm of loose friable alluvium at two locations on the Cooper floodplain; one near Naccowlah Waterhole the other near Durham Downs Station on the Durham Downs Road, 35 km north of Naccowlah (Figure 1.1).

The conditions at the time of collection were quite different. The Naccowlah sediment was taken during a prolonged drought while the Durham Downs sediment was taken soon after a significant wet phase during which the sampling site had been inundated by flood-waters. Despite this, tests showed that the two batches of sediment had similar size and density characteristics.

The sediment samples were sub-divided into batches (A-G) to be used in the flume. Sediment batches obtained from the Naccowlah Waterhole site were labelled Batches A-C; while sediment from the floodplain near Durham Downs were labelled Batches D-G.

## 3.2 Laboratory Flume

The 10 m long, 0.45 m wide and 0.30 m deep flume recirculates both water and sediment, can be adjusted for slope. It is located in the Geography Department at the University of Wollongong (Plate 3.1). The pump is an Ajax

Plate 3.1 General view of the recirculating flume showing the inlet section (right). The channel is 0.45 m wide and 10 m in length.

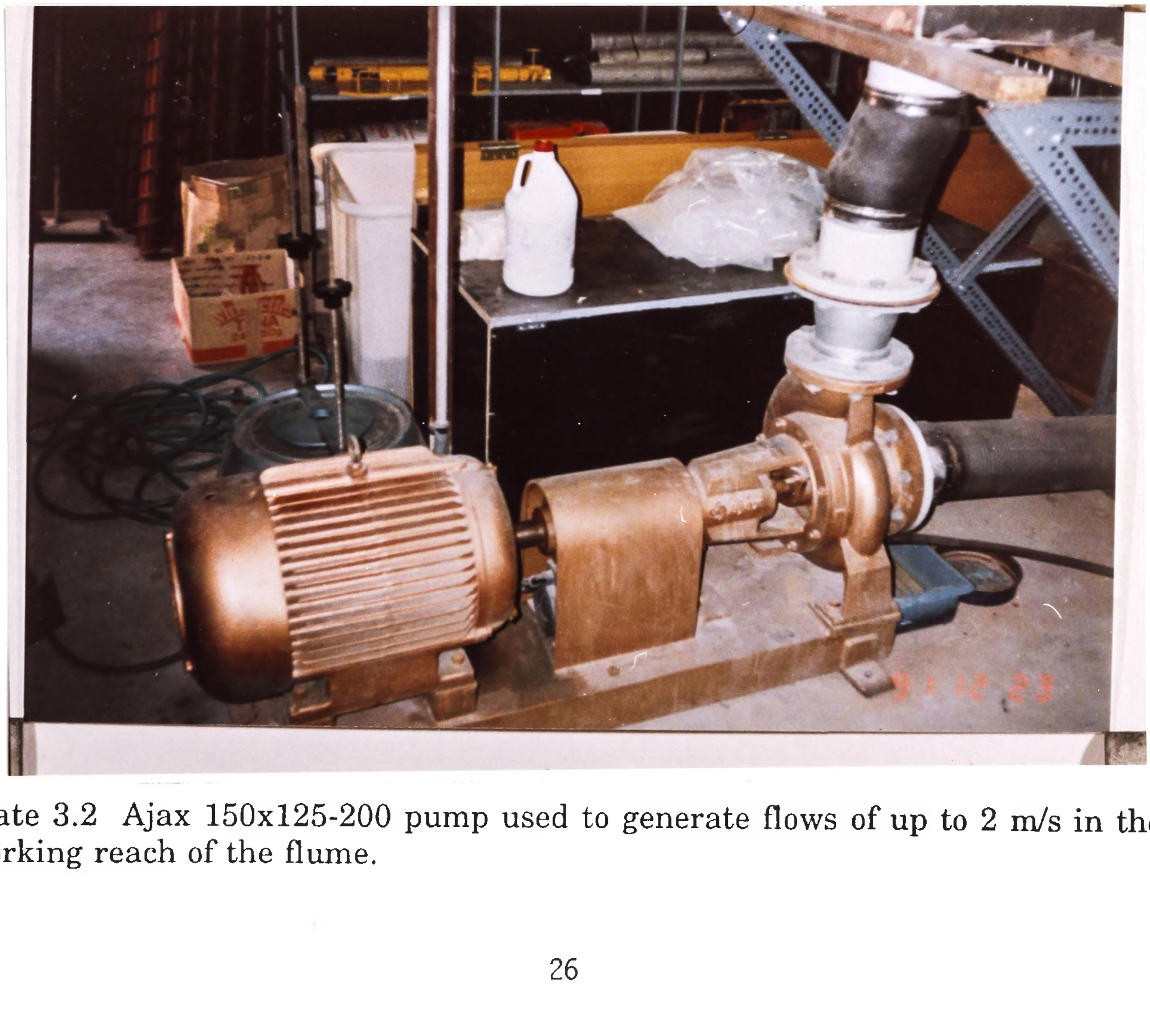

Plate 3.2 Ajax 150x125-200 pump used to generate flows of up to 2 m/s in the working reach of the flume.

150x125-200 with a 960 R.P.M. 2.2 kW electric motor driving a 219 mm impeller which can generate flow velocities of up to 2 $m.s^{-1}$ in the working section of the flume (Plate 3.2).

Due to turbulence arising from flow through the headbox and accelerating flow (drawdown) at the outlet, a 3 m working section in the middle reach of the flume exhibiting steady uniform flow was used to collect data during each experimental run.

## 3.3 <u>Variables measured in the flume</u>

### 3.3.1 Velocity Measurements

A Nixon 403 "Streamflo" current-meter probe was used to measure flow velocities. Plate 3.3 shows both the current meter and instrument panel in position on a moving platform (gantry) above the working reach of the flume. The current-meter probe has an impeller diameter of 0.5 cm enabling it to measure small changes in flow velocity between 0.02 $m.s^{-1}$ and 1.5 $m.s^{-1}$. Therefore, accurate velocity measurements can be made at various depths of flow.

Despite the advantages of such a small and sensitive instrument there was a problem of plant litter (small roots and twigs in the floodplain mud) becoming entangled around the impeller. This made flow velocity measurements very time consuming as the vegetation had to be removed before and during each set of measurements. For this reason a larger current

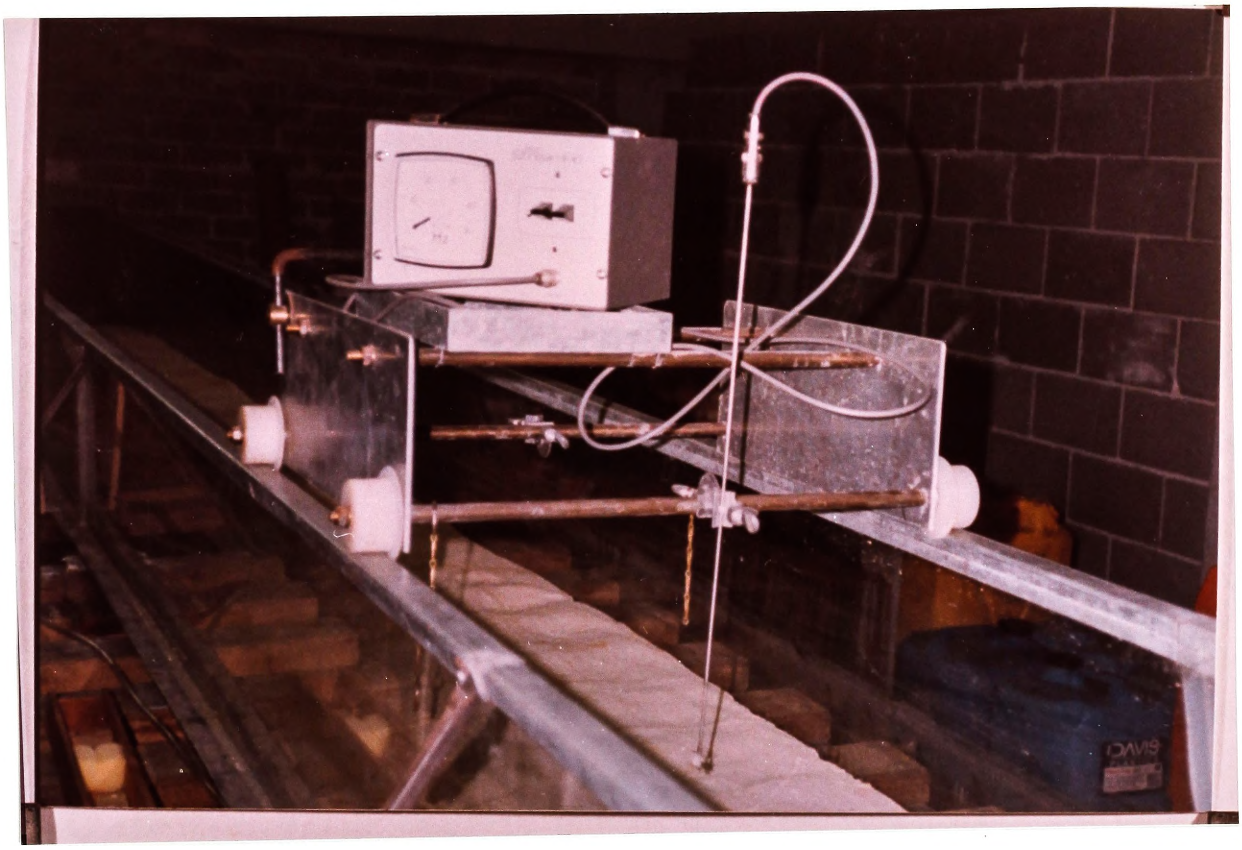

Plate 3.3 Mobile gantry positioned above the flume. The Nixon 403 flow velocity probe and recorder are shown. The probe can be moved both vertically and horizontally in the flow. Flume width = 0.45 m.

meter was sometimes used (Kempten Small Ott Current Meter C2 (10.150)), firstly to check the calibration of the Nixon probe and secondly to obtain velocity measurements under conditions where there was abundant litter in the floodplain sediments. Compared to the Nixon 403 meter the Ott meter has the advantage of shedding debris as it rotates but it lacks the sensitivity to minor fluctuations in velocity and manoeuvrability near the bed of the flume.

Even though the 3 m reach chosen for data collection was relatively free from large-scale turbulence, detailed systematic sampling was undertaken during each experimental run. Two velocity measurements were taken at each of 3 cross-sections at 0.4 times the depth of flow from the bed for every metre of the working section of the flume. Thus a total of 6 measurements were recorded for velocity during each experimental run and these were averaged to obtain a mean value for each set of velocity observations.

### 3.3.2 Depth Measurements

Due to both the presence of bedform undulations and the difficulty in detecting the soft muddy bed with a probe, the measurement of average flow depth was difficult to obtain accurately. Similar problems were encountered by Jopling and Forbes (1979) in an experimental flume study using a glaciofluvial silt. They determined depth of flow from observations through the perspex sidewalls of the flume, a technique adopted here. To ensure a reasonable estimate of flow depth, a total of 12 sidewall observations were recorded during each experimental run. Measurements were made from both sides of the flume at 0.5 m intervals over the 3 m workable reach.

### 3.3.3 Slope Measurements

Using a manometer and point gauges, Jopling and Forbes (1979) acknowledged that water surface slope is the most difficult variable to quantify in small-scale flume experiments. In this study it was measured by using a manometer and by surveying with a dumpy level.

The manometer consisted of plastic tubing connected to a single gradational scale to measure the difference in the elevation of water level at each end of the 3 m working reach of the flume. A problem with the manometer was that it sometimes became clogged with sediment, impairing its accuracy; surveying provided a check and yielded alternative data when the manometer results were inaccurate.

The presence of water-surface waves reduced the accuracy of slopes surveyed during high velocity runs. Under these conditions, several dumpy level values were taken and averaged for each flume run. Water-surface waves did not affect the manometer which acts to dampen the oscillations.

### 3.3.4 Hydraulic parameters calculated using basic flow data

Once average velocity and flow depth were obtained for each run, flow discharge was then computed from width and mean depth. Sidewall corrections (Vanoni and Brooks, 1957) were not necessary in this study given that the depth of flow in the flume did not exceed the limit where wall effects would become significant. The absence of drag is illustrated in Plate 3.4

which shows that the bedforms exhibit no deformation towards the sides, and the depth was also uniform across the flume. Flow depths taken through the perspex sidewalls of the flume are therefore representative of flow depths across the entire section.

Various other parameters were calculated to represent the flow conditions evident in each of the flume experiments. These include the Darcy-Weisbach friction factor, bed shear stress, stream power, Reynold's and Froude numbers (Table 4.3).

### 3.4 Sediment preparation in the flume

The sediment required no elaborate pre-run preparation. It was poured directly on to the dry base of the flume. As would occur on the floodplain, irregularly shaped blocks of aggregated soil were left intact and the surface was roughly levelled in order to have an even layer of dry sediment on the bed prior to introducing water into the flume. Water was allowed to enter the flume and to flow over the sediment on its own accord in much the same way as overbank flow might leave the channels of Cooper Creek and inundate its floodplain. Once a predetermined depth of water had been reached, the pump was started and the flow allowed to equilibrate before data was collected.

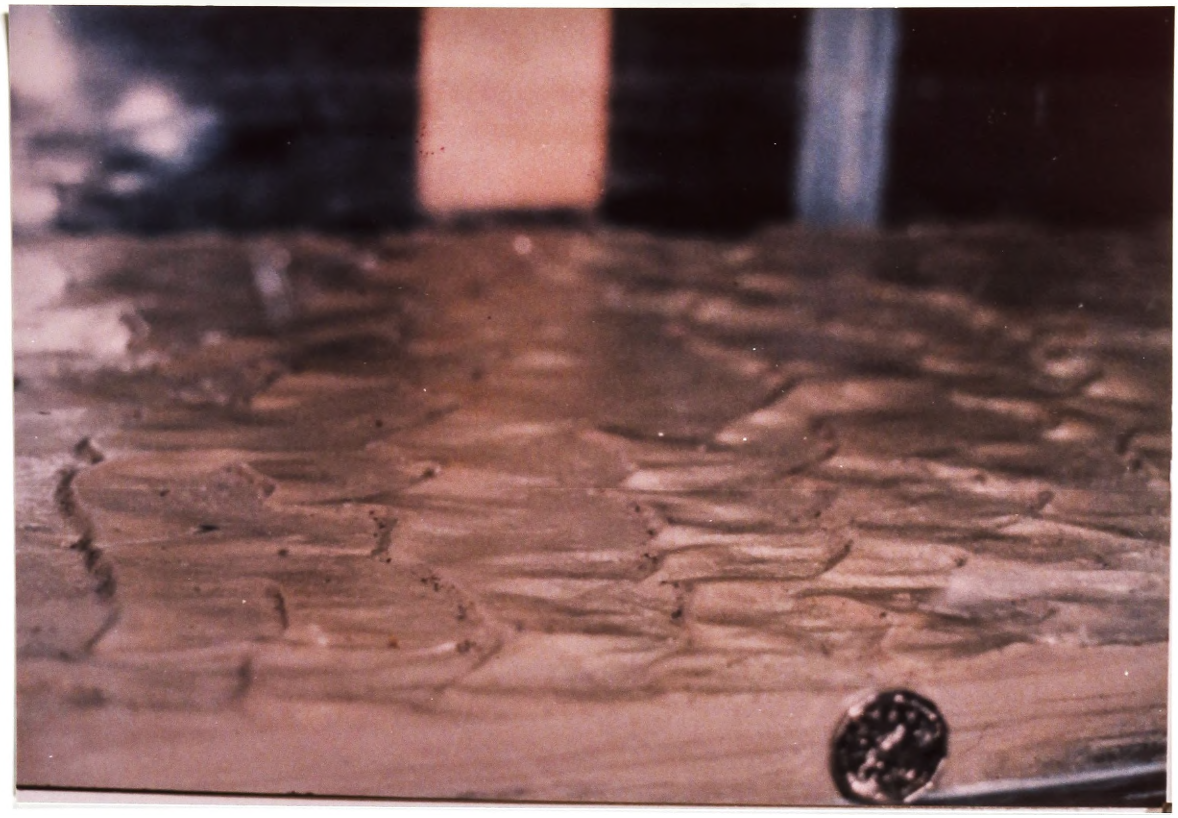

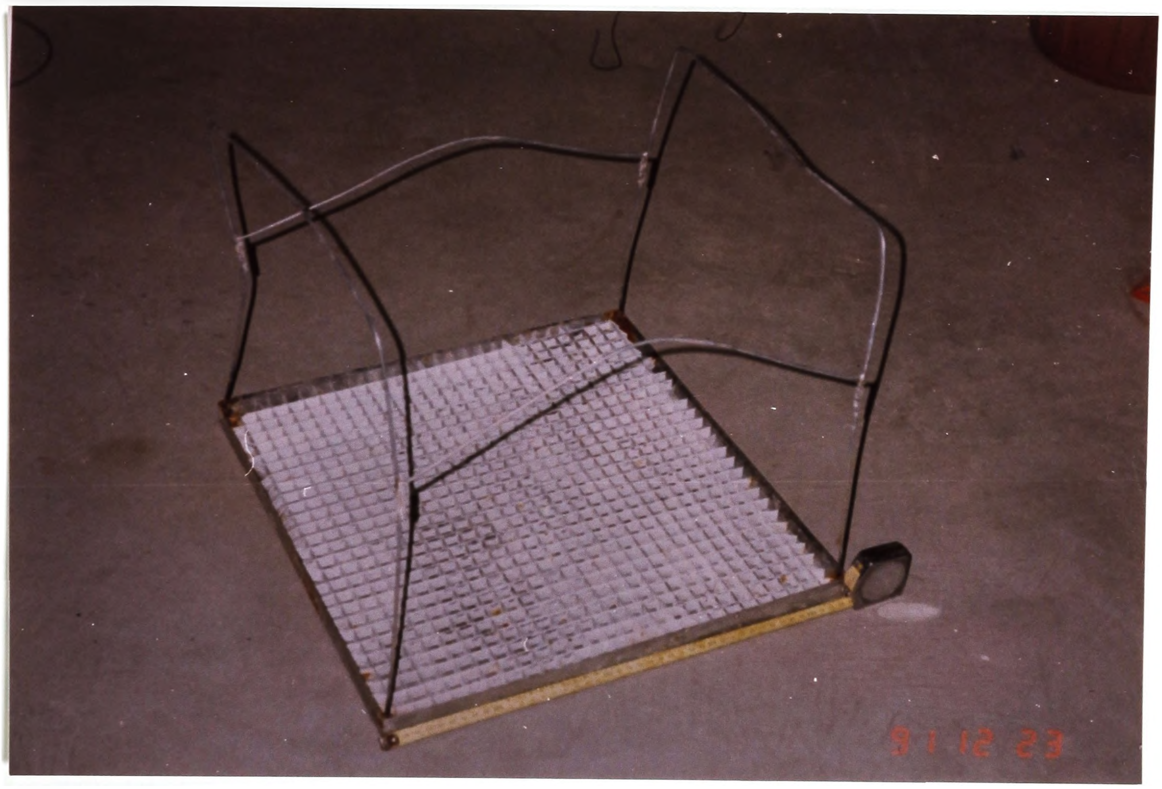


**Plate 3.4 (Top)** Small asymmetrical linguoidal-shaped ripples extending across the entire width of the flume showing that sidewalls do not disrupt bedform development (Run #27). Coin Diameter=0.03 m.

**Plate 3.5 (Bottom)** Bedload trap which was set into the bed of the flume at the end of the 3 m working reach. Width=0.45 m.

## 3.5 Sediment Sampling

### 3.5.1 Suspended load

Using a standard DH 48 suspended sediment sampler, a depth integrated sample was taken from the centre of the flume in the middle of the test reach. Suspended sediment samples were filtered through filter paper, dried and weighed in the laboratory. The product of sediment concentration ($g.l^{-1}$) and flow discharge ($l.s^{-1}$) provides an estimate of the transport rate of suspended sediment per unit time ($g.hr^{-1}$) and per unit flow area ($g.hr^{-1}.m^{-2}$).

### 3.5.2 Bedload transport

Unlike suspended load, bedload is difficult to sample accurately. In this study the problem is accentuated since low-density, relatively fragile muddy sediment cannot be trapped as easily as quartz sand. The latter can be caught in sieves but in this study, there is a problem in determining the transport rates since the sediment is comprised of clay-rich aggregates. Although the aggregates are water stable (Nanson et al., 1986), prolonged soaking of the aggregates and their vibration in a sieve would cause some of them to break down and be lost through the sieves, resulting in an underestimate of bedload. Furthermore, the organic litter in suspension would rapidly clog the sieves and distort the results. As a consequence, another technique was developed to measure the bedload transport rates of the aggregated sediment.

A bedload sediment sampler tray the width of the flume and set at the end of the 3 m working reach was constructed specifically for this purpose. The tray was compartmented with a 45 cm by 35 cm sheet of 1 $cm^2$ 1 cm deep aluminium cubic mesh (Plate 3.5). Thin wire handles extended above the water surface to enable removal of the tray from the flume. The sampler was set below the bed of the flume so that the tray did not adversely affect the flow hydraulics. Sediment moving as bedload fell into the tray and remained trapped within individual compartments of the mesh.

Bedload samples were taken for each experimental run except where no measurable bedload was transported (i.e., at or below incipient motion conditions). The sampling time was controlled by the rate of infilling of the sediment trap which is largely a function of the flow velocity. Little or no sediment was lost at low to moderate flow rates, but at higher rates, where sediment transport rates and flow turbulence was greater, sediment loss during the removal of the tray from the bed probably resulted in some sediment loss. However, the consistent results obtained using this method suggests that the tray sampler provides a useful method for the measurement of bedload transport, even if the maximum values obtained may underestimate the actual transport rates at high discharges.

Sediment collected in the tray after each run was transferred to a container which was placed in an oven to dry at $80^oC$. The dry weight enabled a bedload transport rate ($kg.hr^{-1}$) to be calculated. The transport rate per unit channel width ($kg.hr^{-1}.m^{-1}$) and the average suspended sediment concentration ($g.l^{-1}$) in the flow were also computed. Thus relative rates of sediment transport as suspended and bedload assessed under varying flow conditions. Jopling and Forbes (1979) did not directly measure bedload. They collected suspended sediment samples at the mid-depth of the flume and total sediment concentration at the downstream end of their flume.

## 3.6 Bedform measurements

Bedform dimensions, like depth measurements, were determined from sidewall observations. Evident after draining the flume was that the bedforms near the sidewall were not significantly different in size and shape from those near the centre line, indicating that the smooth perspex sidewalls offered little drag (Plate 3.4).

In addition to rates of bedform movement, the wavelengths and amplitudes of bedforms were recorded over the 3 m working section by taking measurements through both sides of the flume. Values recorded were then averaged so that characteristic bedform dimensions and rates of movement were obtained for each run.

## 3.7 Laboratory Analysis

Determination of the characteristic size distribution of the Cooper Creek sediment was difficult to obtain due to the aggregated nature of the sediment. Size distributions are required to fulfil two functions. Firstly, it is necessary to know the size distribution of the individual clasts (the primary size distribution) comprised largely of individual mineral grains, for it is from these that the sediment aggregates are formed. Size distributions of the individual clastic grains were determined by settling dispersed samples in water and taking measurements with a hydrometer and a pipette. However, most of the sediment is transported as aggregates; therefore the size distribution of aggregated particles was obtained by wet sieving.

### 3.7.1 Hydrometer/Pipette Sediment Size Analysis

The hydrometer method (Bouyoucous, 1928) was used to analyse clastic sediment texture coarser than 0.01 mm and finer than 0.125 mm while the pipette method (Day, 1965) was used (in conjunction with the former) for finer clastic fractions between 0.002 mm and 0.01 mm. An ultrasonic bath was used to aid in the breakdown of the soil aggregates.

### 3.7.2 Wet Sieving Technique

In order to assess soil aggregate size distribution in a manner which causes least disturbance of the aggregate sizes, wet sieving was employed. This involves the gentle agitation of sediment in a nest of sieves immersed in a cylinder filled with water. The sediment is agitated for a period of 15 minutes after which the sieves are separated and the sediment retained in each is washed into containers to be oven dried and weighed.

Prior to wet sieving, the option exists to `wet' the sediment at a designated tension so as to simulate various rates of water application prior to transport (i.e., high tension replicates low-intensity rains and vice versa). Wetting rates with aggregated sediment can dramatically affect the size distribution obtained by wet sieving (Loch and Donnollan, 1983a,b). It is very important that the mode of wetting appropriate to the antecedent conditions experienced by the sediment in the field is applied prior to the commencement of wet sieving. For instance, sediment which is immersion wet (no tension) is placed directly into water. This would in nature simulate overland flow over a dry floodplain. Sediment wet at 2 and 5 cm tension replicates intense and gentle rainfall, respectively (Loch and Donnollan, 1983a,b).

Immersion wetting (no tension) was used in this experiment. As noted earlier, floodwaters from the headwaters of the Cooper system can take several weeks to pass over the floodplains from which this sediment was sampled. Given the arid nature of the climate of the region (<250 mm of rainfall per annum), the possibility of wetting by natural rainfall prior to transport is less likely than total immersion. More often than not, the arrival of a flood wave long after local rainfall has ceased results in the immersion of a dry floodplain surface. Consequently, the samples for this study were subjected to immersion wetting prior to wet sieving.

### 3.7.3 Salinity Measurements

Salinity levels were determined by employing a HACH salinity meter probe. Samples were prepared to a standard set out by the United States Department of Agriculture (Richards, 1954). Salinity measurements were collected for each of the 7 sediment batches that were used in the flume. In addition, a salinity sample was taken of water from one of the channels of the Cooper on the falling stage of a recent flood.

### 3.7.4 Sediment Density

Two techniques were used to measure sediment density; the standard kerosene method and an alternative using water. The latter was used as a check on the former as it was thought that kerosene may break down the sediment aggregates, however, there was no discernible difference in the values obtained using each.

### 3.7.5 Wetting/Drying Investigation

A simple laboratory investigation was conducted to examine the development of aggregates from dispersed sediment. The experiment involved simulating microclimatic conditions on the floodplain of Cooper Creek to determine how rapidly and under what conditions the floodplain soils will aggregate.

A sample of the original aggregated sediment was mixed with distilled water and dispersed using an ultrasonic bath. It was then dried under an infra-red lamp (to simulate drying and heating by the sun) before being immersed in distilled water (to simulate rainfall or flooding). This wetting and drying was repeated several times and changes in sediment structure were observed.

# CHAPTER 4 RESULTS OF SEDIMENT ANALYSIS AND FLUME EXPERIMENTS.

## 4.1 Sediment Characteristics

The tests outlined in Chapter 3 were undertaken to determine the primary (non-aggregated) texture and the aggregated texture of the sediment being used in the laboratory flume. Particle size, density and salinity values are presented below in Table 4.1.

### 4.1.1 Evaluation of sediment size

Non-aggregated particle size analysis of the two batches of sediment used in this study using the hydrometer/pipette methods of analysis revealed that approximately 63% of the aggregated sediment is composed of clay with the remainder being comprised mostly of fine sand with some silt and coarse sand (Table 4.1).

Results from the wet-sieving of both batches of sediment samples are presented in Table 4.1 for 3 different wetting rates and show the effects of wetting rates on median aggregate diameter.

Nanson et al. (1986), obtained a median particle size of 0.125 mm in Cooper floodplain sediments collected at Naccowlah using immersion wet samples, but with a less accurate wet sieving technique than that used in this study. Both sediment samples from this study have the same median sediment diameter of 0.10 mm when immersion wet (Figure 4.1), however, the differences in size with different wetting rates is dramatic. Tension wet

| Cooper Creek Sediment Analysis | | |
|---|---|---|
| *** Particle Sizes Analysis** | | |
| | **Naccowlah Waterhole (Batches A-C)** | **Durham Downs (Batches D-G)** |
| | (%) | |
| Coarse Sand and Medium Sand | 3.5 | 4.1 |
| Fine Sand | 24.9 | 23.7 |
| Silt | 8.9 | 8.8 |
| Clay | 62.7 | 63.4 |
| *** Median Aggregate Size ($d_{50}$)** | | |
| | (mm) | |
| Immersion Wetting | 0.10 | 0.10 |
| Tension Wetting at 2 cm | 0.60 | 0.80 |
| Tension Wetting at 5 cm | 0.80 | 0.90 |
| *** Sediment Parameters (Folk, 1968)** | | |
| Sorting Index, $S_o$ | 0.11 | 0.14 |
| Skewness Index, $S_g$ | 0.55 | 0.51 |
| Kurtosis Index, $K_g$ | 1.32 | 1.44 |
| *** Salinity Levels** | | |
| | 150-200 ppm (<0.02%) | |
| *** Density (aggregates)** | | |
| | ($kg.m^{-3}$) | |
| | 2310 | 2270 |
| | | **TABLE 4.1** |

samples are almost an order of magnitude larger in aggregate median diameter. As stated in Chapter 3, the justification for the use of immersion wetting is that these floodplain sediments are transported usually by the passage of a floodwave over a previously dry floodplain.

Cumulative plot of aggregate size distribution for both sediment batches

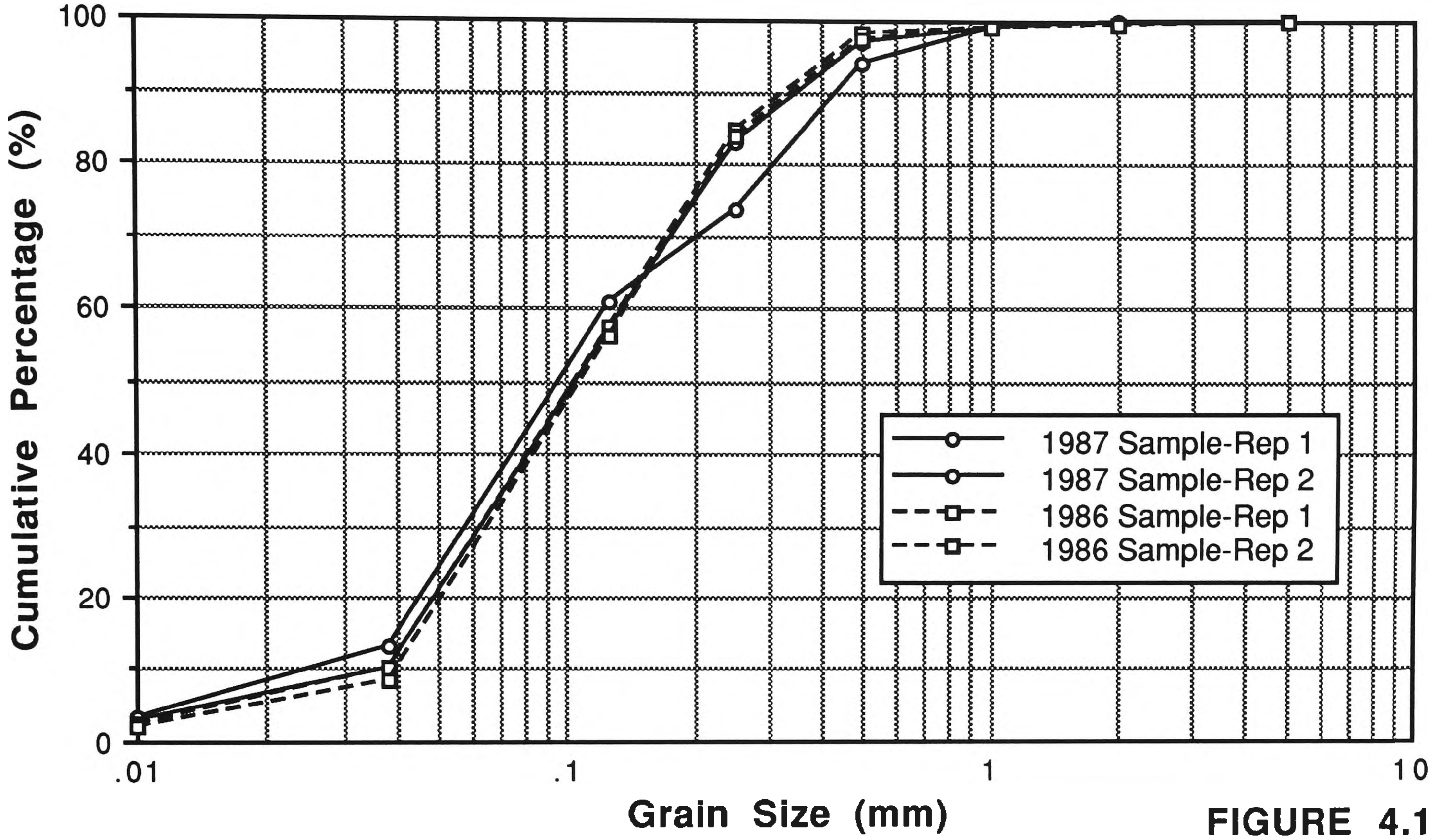


FIGURE 4.1

During the flume experiments, results were collected quickly once equilibrium flow conditions were attained. This minimised the degree of comminution of the aggregated sediment caused by both prolonged immersion in water and the effect of intense turbulence caused by the pump's impeller.

### 4.1.2 Density Measurements

The Naccowlah sediment was slightly less dense than the Durham Downs samples (Table 4.1), but the range of variation was not seen as significant (2270-2310 $kg.m^{-3}$). Nanson et al. (1986) reported an aggregate density of 2310 $kg.m^{-3}$ which agrees closely with the values for both batches (Table 4.1). In calculations employing aggregate density, a value of 2300 $kg.m^{-3}$ was used, significantly lower than that of quartz sand (2660 $kg.m^{-3}$).

### 4.1.3 Salt (NaCl) Measurements

Salt (NaCl) levels for the sediment were found to be very low (< 0.02% by weight; Table 4.1), a result consistent with other independent reports on sediment from the Cooper floodplain (Ogilve, 1948; Dawson and Ahern, 1974; Nanson et al., 1986). Given the arid nature of the Eyre Basin, the prevalence of saline lakes in the region and the abundance of calcrete and gypcrete in the subsoil (below about 2 m; Nanson et al., 1988) the low solute content of the surface 0.5-1.0 m of the floodplain is perhaps surprising, however, rainfall and flooding probably flush the surface sediments clean of most soluble salts. A salinity sample taken during the falling stage of a recent flood event on the Cooper was found to have a salt concentration of 85 ppm.

The absence of salt in the aggregated sediment has important implications for the way aggregates in this environment are formed (Bowler, 1973; Nanson et al., 1988).

## 4.2 Flume Results

A total of 33 flume runs (using 7 sediment changes) were performed during this study. Sediment changes were necessary as turbulence from the impeller in the pump assisted in disaggregating sediment during transport.

A wide range of flow conditions were simulated in the flume. Discharges ranged between 1.8 and 30.2 $l.s^{-1}$, mean velocities between 4 and 69 $cm.s^{-1}$, flow depths between 4 and 12 cms and slopes between 0.0002 and 0.0041 $m.m^{-1}$. Table 4.2 presents the results of the basic flow data obtained for the 33 runs using several sediment batches. Computed flow parameters using data from Table 4.2 are given in Table 4.3.

Calculations in Table 4.3 assume the following: g (gravity)=9.81 $m.s^{-2}$, $\upsilon$ (viscosity)=$10^{-6}$ $kg.m^{-1}.s^{-1}$ at 20°C and $\rho$ (density of water)=1000 $kg.m^{-3}$ at 20°C. Variations in water temperature occurred between and during each experimental run but were not sufficient to be regarded as a significant variable. Viscosity changes due to changing suspended sediment concentration were probably more significant but have not been included in the analyses and therefore may account for some of the variability in results.

| Basic Flow and Sediment Discharge Data | | | | | | | | |
|---|---|---|---|---|---|---|---|---|
| Run Number | Bedform | Flow Discharge ($l.s^{-1}$) | Mean Depth (cm) | Mean Velocity ($cm.s^{-1}$) | Water Surface Slope ($m.m^{-1}$) | Temp. ($^oC$) | Bedload ($g.s^{-1}$) | Suspended Load ($g.l^{-1}$) |
| | | **Q** | **d** | $\upsilon$ | **s** | **T** | $C_b$ | $C_s$ |
| **BATCH A** | | | | | | | | |
| 1 | Ripples | 20.4 | 8.7 | 52.0 | 0.002 | 23.0 | n/a | n/a |
| 2 | Ripples | 30.2 | 12.0 | 56.1 | 0.001 | 20.0 | n/a | n/a |
| **BATCH B** | | | | | | | | |
| 3 | Ripples | 3.8 | 6.5 | 13.0 | 0.002 | 23.0 | 0.00 | 0.06 |
| 4 | Ripples | 18.6 | 6.0 | 69.0 | 0.002 | 23.0 | n/a | 42.60 |
| **BATCH C** | | | | | | | | |
| 5 | Ripples | 2.7 | 9.8 | 6.2 | 0.002 | 20.0 | 0.00 | 0.46 |
| 6 | Ripples | 3.8 | 10.5 | 8.0 | 0.002 | 20.0 | 0.00 | 0.43 |
| 7 | Ripples | 5.7 | 10.5 | 12.3 | 0.002 | 20.5 | 0.10 | 0.28 |
| 8 | Ripples | 13.5 | 10.7 | 28.0 | 0.002 | 21.0 | 0.10 | 3.00 |
| 9 | Ripples | 17.1 | 10.0 | 37.8 | 0.001 | 21.0 | 0.33 | 8.40 |
| 10 | Plane Bed (LR) | 2.1 | 11.4 | 4.1 | 0.001 | 20.5 | 0.00 | 0.00 |
| **BATCH D** | | | | | | | | |
| 11 | Plane Bed (LR) | 1.8 | 9.8 | 4.3 | 0.001 | 21.0 | 0.00 | 0.30 |
| 12 | Ripples | 3.1 | 9.7 | 7.2 | 0.001 | 21.0 | 0.00 | 0.55 |
| 13 | Ripples | 4.3 | 9.5 | 10.2 | 0.001 | 21.0 | 0.23 | 0.77 |
| 14 | Ripples | 13.4 | 8.3 | 36.0 | 0.001 | 22.0 | 0.89 | 8.81 |
| 15 | Ripples | 4.3 | 5.6 | 16.9 | 0.001 | 24.0 | 4.50 | 5.30 |
| 16 | Ripples | 3.4 | 4.5 | 17.1 | 0.002 | 24.0 | 2.41 | n/a |
| 17 | Ripples | 5.0 | 4.0 | 28.3 | 0.001 | 25.0 | 1.29 | n/a |
| 18 | Ripples | 9.9 | 4.7 | 47.4 | 0.002 | 22.0 | 11.35 | 7.34 |
| 19 | Antidunes | 14.6 | 5.4 | 59.9 | 0.004 | 24.0 | 15.18 | 8.51 |
| **BATCH E** | | | | | | | | |
| 20 | Plane Bed (UR) | 14.9 | 5.5 | 60.2 | 0.003 | 22.0 | 18.00 | 8.42 |
| 21 | Plane Bed (UR) | 19.1 | 5.5 | 77.1 | 0.003 | 22.0 | 24.04 | 16.92 |
| **BATCH F** | | | | | | | | |
| 22 | Ripples | 4.7 | 6.5 | 16.0 | 0.002 | 15.5 | 7.97 | 9.78 |
| 23 | Ripples | 7.1 | 6.6 | 24.2 | 0.002 | 16.5 | 15.62 | 33.63 |
| 24 | Ripples | 9.8 | 7.5 | 29.4 | 0.001 | 17.5 | 30.05 | 54.59 |
| 25 | Ripples | 9.8 | 5.9 | 37.2 | 0.002 | 16.0 | 63.26 | 121.71 |
| 26 | Ripples | 11.2 | 5.8 | 43.0 | 0.004 | 17.0 | 63.64 | 230.90 |
| 27 | Ripples | 5.5 | 10.2 | 12.3 | 0.001 | 15.5 | 0.00 | 0.21 |

| Basic Flow and Sediment Discharge Data (continued) | | | | | | | | |
|---|---|---|---|---|---|---|---|---|
| Run Number | Bedform | Flow Discharge ($l.s^{-1}$) | Mean Depth (cm) | Mean Velocity ($cm.s^{-1}$) | Water Surface Slope ($m.m^{-1}$) | Temp. ($^{o}C$) | Bedload ($g.s^{-1}$) | Suspended Load ($g.l^{-1}$) |
| | | **Q** | **d** | $\upsilon$ | **s** | **T** | $C_b$ | $C_s$ |
| **BATCH G** | | | | | | | | |
| 28 | Ripples | 8.0 | 9.3 | 18.9 | 0.001 | 16.0 | 0.32 | 0.72 |
| 29 | Ripples | 6.9 | 8.5 | 18.1 | 0.001 | 17.5 | 0.78 | 1.40 |
| 30 | Ripples | 11.3 | 9.3 | 27.0 | 0.001 | 18.0 | 3.35 | 3.43 |
| 31 | Ripples | 10.8 | 8.6 | 28.3 | 0.001 | 20.5 | 5.13 | 24.47 |
| 32 | Ripples | 11.0 | 5.7 | 42.8 | 0.002 | 16.0 | 37.07 | 24.04 |
| 33 | Plane Bed (UR) | 17.2 | 6.7 | 57.0 | 0.003 | 16.5 | 90.69 | 63.24 |

**Note:** Flume width = 45 cm UR=Upper Regime LR=Lower Regime n/a=not available

**TABLE 4.2**

**Parameters derived from Basic Flow Data**

| Run Number | Cross-Sectional Area (cm²) | Hydraulic Radius (cm) | Darcy-Weisbach Friction Factor | BedShear Stress (kg.m⁻¹.s⁻²) | Stream Power (N.m⁻¹.s⁻¹) | Reynold's Number | Froude Number |
|---|---|---|---|---|---|---|---|
| | **A** | **r** | **f** | $\tau$ | $\tau.\upsilon$ | **Re** | **Fr** |
| **BATCH A** | | | | | | | |
| 1 | 391.5 | 6.3 | 0.05 | 1.71 | 0.89 | 32760 | 0.56 |
| 2 | 540.0 | 7.8 | 0.04 | 1.41 | 0.79 | 43758 | 0.52 |
| **BATCH B** | | | | | | | |
| 3 | 292.5 | 5.0 | 0.69 | 1.47 | 0.19 | 6500 | 0.16 |
| 4 | 270.0 | 4.7 | 0.02 | 1.18 | 0.81 | 32430 | 0.90 |
| **BATCH C** | | | | | | | |
| 5 | 441.0 | 6.8 | 0.40 | 0.19 | 0.01 | 4216 | 0.06 |
| 6 | 472.5 | 7.2 | 0.26 | 0.21 | 0.01 | 5760 | 0.08 |
| 7 | 472.5 | 7.2 | 0.11 | 0.21 | 0.03 | 8856 | 0.12 |
| 8 | 481.5 | 7.3 | 0.02 | 0.21 | 0.06 | 20440 | 0.27 |
| 9 | 450.0 | 6.9 | 0.06 | 0.98 | 0.37 | 26082 | 0.38 |
| 10 | 513.0 | 7.6 | 1.60 | 0.34 | 0.01 | 3116 | 0.04 |
| **BATCH D** | | | | | | | |
| 11 | 441.0 | 6.8 | 0.83 | 0.19 | 0.01 | 2924 | 0.04 |
| 12 | 436.5 | 6.8 | 0.29 | 0.19 | 0.01 | 4896 | 0.07 |
| 13 | 427.5 | 6.7 | 0.14 | 0.19 | 0.02 | 6834 | 0.11 |
| 14 | 373.5 | 6.1 | 0.01 | 0.16 | 0.06 | 21960 | 0.40 |
| 15 | 252.0 | 4.5 | 0.15 | 0.55 | 0.09 | 7605 | 0.23 |
| 16 | 202.5 | 3.8 | 0.28 | 1.01 | 0.17 | 6498 | 0.26 |
| 17 | 180.0 | 3.4 | 0.04 | 0.39 | 0.11 | 9622 | 0.45 |
| 18 | 211.5 | 3.9 | 0.04 | 1.06 | 0.50 | 18486 | 0.70 |
| 19 | 243.0 | 4.4 | 0.05 | 2.17 | 1.30 | 26356 | 0.82 |
| **BATCH E** | | | | | | | |
| 20 | 247.5 | 4.4 | 0.04 | 1.62 | 0.97 | 26488 | 0.82 |
| 21 | 247.5 | 4.4 | 0.02 | 1.62 | 1.25 | 33924 | 1.05 |
| **BATCH F** | | | | | | | |
| 22 | 292.5 | 5.0 | 0.40 | 1.27 | 0.20 | 8000 | 0.20 |
| 23 | 297.0 | 5.1 | 0.18 | 1.29 | 0.31 | 12342 | 0.30 |
| 24 | 337.5 | 5.6 | 0.07 | 0.74 | 0.22 | 16464 | 0.34 |
| 25 | 265.5 | 4.7 | 0.08 | 1.33 | 0.50 | 17484 | 0.49 |
| 26 | 261.0 | 4.6 | 0.09 | 2.10 | 0.91 | 19780 | 0.57 |
| 27 | 459.0 | 7.0 | 0.16 | 0.30 | 0.04 | 8610 | 0.12 |

| Parameters derived from Basic Flow Data (continued) | | | | | | | |
|---|---|---|---|---|---|---|---|
| Run Number | Cross-Sectional Area ($cm^2$) | Hydraulic Radius (cm) | Darcy-Weisbach Friction Factor | BedShear Stress ($kg.m^{-1}.s^{-2}$) | Stream Power ($N.m^{-1}.s^{-1}$) | Reynold's Number | Froude Number |
| | **A** | **r** | **f** | $\tau$ | $\tau.\upsilon$ | **Re** | **Fr** |
| **BATCH G** | | | | | | | |
| 28 | 418.5 | 6.6 | 0.06 | 0.27 | 0.05 | 12474 | 0.20 |
| 29 | 387.0 | 6.2 | 0.14 | 0.58 | 0.11 | 11222 | 0.20 |
| 30 | 418.5 | 6.6 | 0.10 | 0.91 | 0.25 | 17820 | 0.28 |
| 31 | 387.0 | 6.2 | 0.06 | 0.59 | 0.17 | 17546 | 0.31 |
| 32 | 256.5 | 4.6 | 0.05 | 1.12 | 0.48 | 19688 | 0.57 |
| 33 | 301.5 | 5.2 | 0.04 | 1.71 | 0.97 | 29640 | 0.70 |
| **NOTE:** Specific gravity of sediment = 2300 $kg.m^{-3}$ | | | | | | | **TABLE 4.3** |

## 4.3 Bedform development and migration rates.

One of the unique properties of this aggregated sediment is its inherent ability to develop primary depositional bedform structures. For a range of flow conditions, a wide spectrum of bedforms were observed including plane bed (with no bedload movement), incipient motion on a plane bed, ripples, plane bed (transitional) and antidunes. Some of these bed states are illustrated below in Figures 4.1 and 4.2. Table 4.2 presents data on the types of bedforms produced in the flume while Table 4.4 presents the migration rates of the sedimentary structures.

The criteria used to seperate the lower regime bedform states of ripples and dunes has been outlined earlier in Chapter 2. In some instances the bedforms were not easily identified when the bedforms were in a transitional phase.

Peak bedform migration rates of 3.9 and 3.5 $m.hr^{-1}$ were measured for Runs 32 and 33, respectively. Although the bedforms evident in Run 33 were categorised as plane bed, some remnant dune features present allowed the measurement of migration rates.

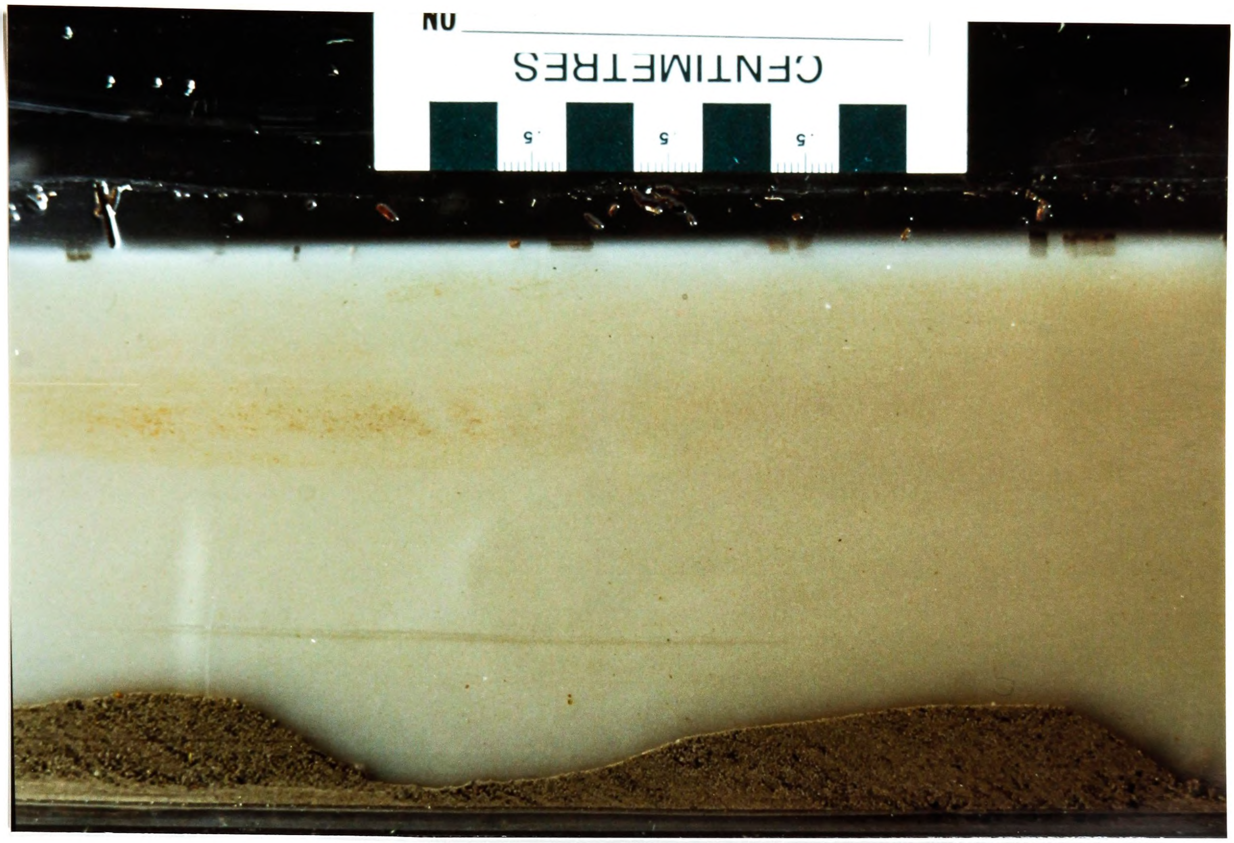

**Plate 4.1 (Top)** Asymmetrical ripples showing well-developed foreset laminae (Run #23). Scale divisions 1 cm long.

**Plate 4.2 (Bottom)** Ripple showing primary form-discordant or composite structure (Run #26). Scale divisions 1 cm long.

| Bedform Dimensions and Migration Rates | | | | | |
|---|---|---|---|---|---|
| Run No. | Migration Rate (cm.hr$^{-1}$) | Mean Bedform Dimensions | | | Bedform |
| | | Amplitude (H) (cm) | Wavelength ($\lambda$) (cm) | $\lambda.H^{-1}$ (-) | |
| 1 | - | - | - | - | Ripples |
| 2 | - | 2.5 | 10.0 | 4.0 | Ripples |
| 3 | 40.0 | 2.0 | 20.3 | 10.2 | Ripples |
| 4 | 30.0 | 1.5 | 25.0 | 16.7 | Ripples |
| 5 | < 0.5 | 0.1 | 0.5 | 5.0 | Ripples |
| 6 | < 0.5 | 0.2 | 3.0 | 15.0 | Ripples |
| 7 | 0.5 | 0.2 | 11.0 | 55.0 | Ripples |
| 8 | 11.1 | 1.4 | 8.5 | 6.1 | Ripples |
| 9 | 49.6 | - | - | - | Ripples |
| 10 | 0.3 | < 0.1 | - | - | Plane Bed (lower regime) |
| 11 | < 0.5 | < 0.1 | - | - | Plane Bed (lower regime) |
| 12 | < 0.5 | < 0.1 | - | - | Ripples |
| 13 | < 0.5 | < 0.1 | - | - | Ripples |
| 14 | < 0.5 | 0.3 | 4.0 | 13.3 | Ripples |
| 15 | 1.2 | 2.6 | 16.1 | 6.2 | Ripples |
| 16 | 6.8 | 1.8 | 9.9 | 5.5 | Ripples |
| 17 | 13.8 | 2.0 | 10.5 | 5.3 | Ripples |
| 18 | - | - | - | - | Ripples |
| 19 | - | - | - | - | Antidunes |
| 20 | - | - | - | - | Plane Bed (upper regime) |
| 21 | - | - | - | - | Plane Bed (upper regime) |
| 22 | 72.0 | 1.9 | 15.0 | 7.9 | Ripples |
| 23 | 102.0 | 1.9 | 12.9 | 6.8 | Ripples |
| 24 | 138.0 | 2.2 | 15.1 | 6.9 | Ripples |
| 25 | 140.0 | 1.6 | 14.1 | 8.8 | Ripples |
| 26 | 130.0 | 2.3 | 22.0 | 9.6 | Ripples |
| 27 | 3.7 | 0.2 | 2.3 | 11.5 | Ripples |
| 28 | 39.0 | 1.7 | 9.4 | 5.5 | Ripples |
| 29 | 21.0 | 2.8 | 14.8 | 5.3 | Ripples |
| 30 | 42.0 | 2.1 | 12.4 | 5.9 | Ripples |
| 31 | 42.0 | 2.0 | 13.9 | 7.0 | Ripples |
| 32 | 348.0 | 1.6 | 11.8 | 7.4 | Ripples |
| 33 | 394.0 | 1.3 | 12.2 | 9.4 | Plane Bed (upper regime) |

**TABLE 4.4**

Figure 4.2 presents a plot of the bedform amplitude (H), bedform wavelength ($\lambda$) and the ratio wavelength/amplitude ($\lambda.H^{-1}$) against Froude Number. A similar diagram was presented by Jopling and Forbes (1979) for a fine fluvioglacial sediment. They suggested that Froude number is a useful indicator of bedform size and bed relief. Also, they found wavelength is relatively insensitive to Froude number but bedform amplitude and $\lambda.H^{-1}$ show broad stable maximums for Froude numbers between 0.4 and 0.6. A high degree of scatter is evident in Figure 4.2. The only similarity being a band for $\lambda.H^{-1}$ of between 5 and 15 exists for Froude numbers between 0.2 and 0.6.

Very little bedform development for fine-grained sediment has been observed in upper regime flow apart from this study and that of Jopling and Forbes (1979). Ripples of varying scales formed readily in the aggregated muds of this study. Since the aggregated sediment behaved as fine sand-sized grains, the resulting bedforms are similar to those formed of sand in the clastic study by Simons and Richardson (1966).

### 4.3.1 Some unusual bedform features observed in the flume.

Several deep scour holes (2-3 cm deep) were observed through the sidewalls in Run #3 as shown in Plate 4.3. This illustrates the cohesive nature of the aggregated sediment a feature not evident in quartz sands. These scour holes are probably caused by small boils on the water surface. There is considerable similarity between these scour features and those observed by Jopling and Forbes (1979).

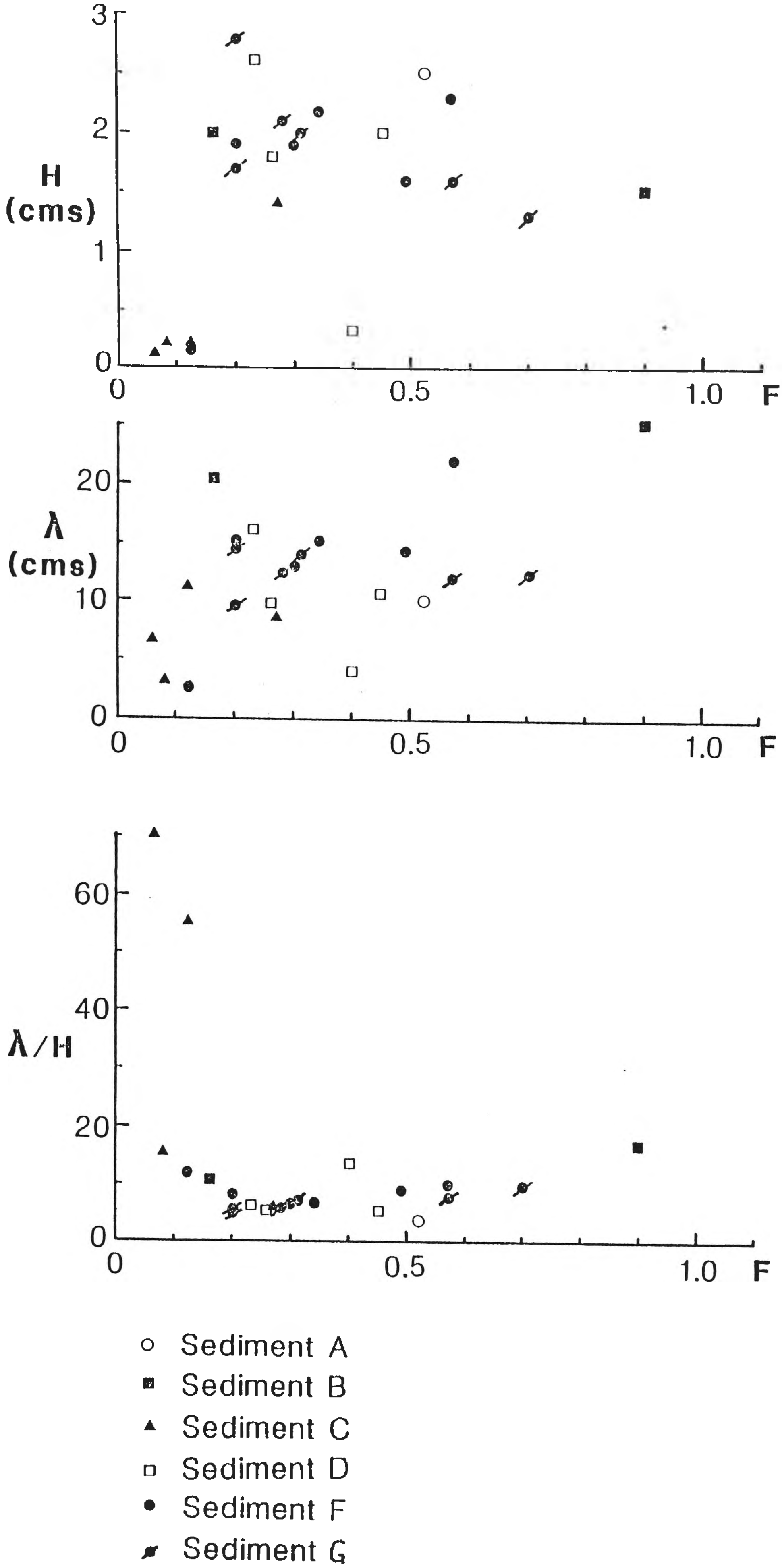


Figure 4.2 Relationship between bedform size indices (height H, length λ and λ/H) and Froude Number.

In one flume run (Run #17) a low amplitude ripple has been completely encased by a larger ripple (Plate 4.4). This occurred towards the end of an experimental run where the sediment was exposed to the flow for many hours and then the flow rate was suddenly increased. The smaller, encased ripple maintained its original form.

During extended periods of transport some of the sediment disaggregates thereby placing higher concentrations of clay into suspension. With fluctuating flow conditions, some of this suspended load coats the bed with a cohesive skin or 'clay-armour'. This resistant skin of fine sediment is visible in Plate 4.4 draped over the original laminae bedding planes and the loosely deposited aggregates of the encased ripple. The larger enclosing ripple is more compacted, finer grained and with no obvious bedding planes, possible as a result of comminution of the sediment aggregates over time.

In all other flume runs where the flow velocity was increased early in a run, the bedforms changed readily in response to the altered hydraulic conditions. It was important to collect the necessary data before comminution of sediment occurred.

Plate 4.3 Deep scourhole located behind a small climbing ripple (centre) which trails a larger ripple (Run 3). Flow is from left. Scale: 1 unit = 1 cm.

Plate 4.4 Small low amplitude ripple encased by a larger, compacted ripple (Run 17). Aggregates are clearly evident in the smaller ripple but not in the larger ripple.

In Run #31, a velocity of 28 $cm.s^{-1}$ and flow discharge of 10.8 $l.s^{-1}$ was maintained for a period of 28 hours. During this period ripples developed and migrated downstream at a rate of 42 $cm.hr^{-1}$. In the first 18-22 hours the ripples appeared hummocky as rounding of the upstream and downstream sides of the ripples took place. The bed then became more compacted, reducing the proportion of loosely packed aggregates and entrapped air pockets. After 22 hours, a very resistant grey-coloured clay layer with an average thickness of 0.8 cm formed over the entire surface of the bed. This clay layer draped a gently undulating surface making it very resistant to changes in flow conditions. The clay drape was very smooth to touch, required force to penetrate and acted as a `clay-armour' protecting the coarser aggregates beneath.

### 4.3.2 Bedform Existence Diagrams

The clay aggregates from the Cooper floodplain developed primary bedform structures typical of sedimentary structures formed by sand-sized quartz grains. Bedform stability diagrams have been developed to graphically describe the connection between flow conditions and associated bedforms (Southard and Boguchwal, 1990). Details of bedform existence diagrams was given earlier in Chapter 2.

Figure 4.3 is one such bedform stability diagram which presents the relationship between flow velocity (standardised to $10^{o}C$) and grain size for 3 ranges of flow depth (standardised to $10^{o}C$). The lines on the graphs represent

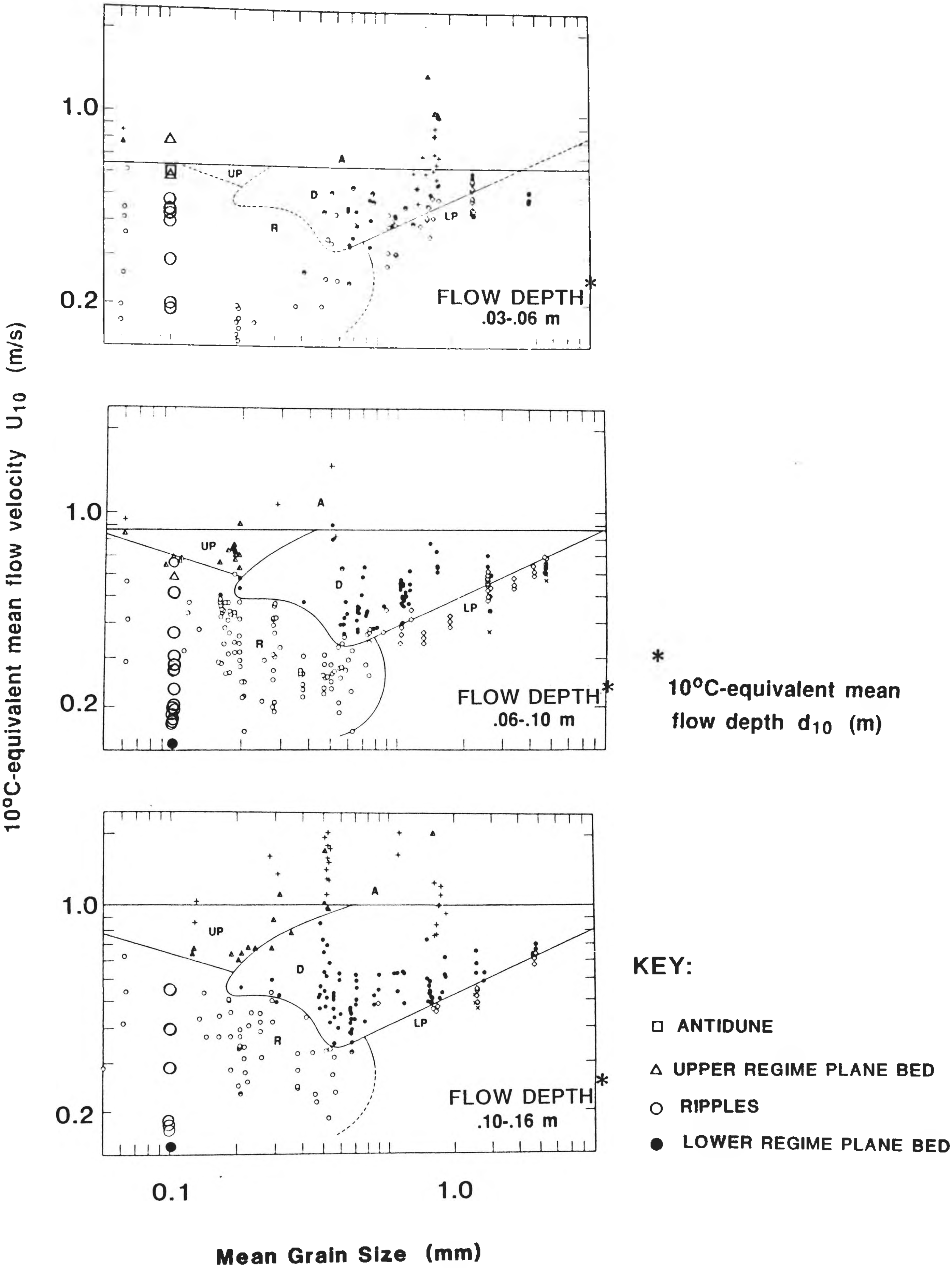


**FIGURE 4.3** Plot of 10°C-equivalent mean flow depth d10 versus 10°C-equivalent mean flow velocity U10 for median sediment sizes in the range of 0.10-0.14 mm. NM=no movement; R=ripples; D=dunes; LP=lower regime plane bed; UP=upper-regime plane bed; A=antidunes. (Modified from Southard and Boguchwal, 1990).

boundaries between various bed states. These boundaries have been developed from an extensive data source involving 39 other flume studies of steady, unidirectional flows (Southard and Boguchwal, 1990). Some of these data points are included in Figure 4.3. Data for all 33 experimental flume runs in this study are plotted to examine their correspondence with the bed phases shown in Figure 4.3.

In general all points lie well within the expected bedform boundaries demarcating the bedform categories for equivalent sized quartz grains. Upper regime plane beds and antidunes in general plot in the appropriate regions of the diagram. All ripple bedforms conform to the bed phases shown on the diagram but no information is given about the transition between the ripple bed state and the lower regime plane bed (no motion). Therefore, this diagram is of little use in assessing both the bedforms at this transition (between ripples and lower regime plane beds) and also the critical threshold of entrainment for the aggregated sediment. Therefore another more applicable bedform stability diagram will be examined in a later section to address this issue.

## 4.4 Rates of Sediment Transport

Bedload and suspended sediment discharge measurements were recorded for all experimental runs except where incipient motion conditions were examined.

### 4.4.1 Initiation of Sediment Transport

Given that the aggregates have a relatively low density compared to quartz sands of similar size, it is plausible that the entrainment threshold of the material would also be quite low. Initially, this aspect was examined by considering the Shield's entrainment curve (Allen, 1985a). It was soon clear that this approach would not be appropriate for this study. The primary reason being that considerable errors in determining slope in the flume (as described earlier in Chapter 3) would be introduced into the dimensionless shear stress expression. Similar problems in determining slope were identified by Jopling and Forbes (1979). Therefore using values for dimensionless shear stress would not be representative of threshold entrainment conditions for the aggregated sediment in the flume.

Therefore, an alternative, more physically based method was used to examine the lower entrainment thresholds for the sediment. Southard and Boguchwal (1990) developed a series of bedform stability diagrams using data from 39 flume studies. Their work represents the most current available information relating various bedform states to hydraulic conditions in steady, unidirectional water flows. Figure 4.4 in particular is useful as it is representative of the relationships among the various bed-phases. It presents a depth-velocity diagram (standardised to $10^{o}C$) for sediment sizes in the range of 0.10-0.14 mm. Data from some of the 39 other flume studies are shown along with the boundaries between the various bed phases. Figure 4.4 also clearly defines the region of no motion (NM) which is of particular interest in examining the entrainment threshold of the aggregated sediment.

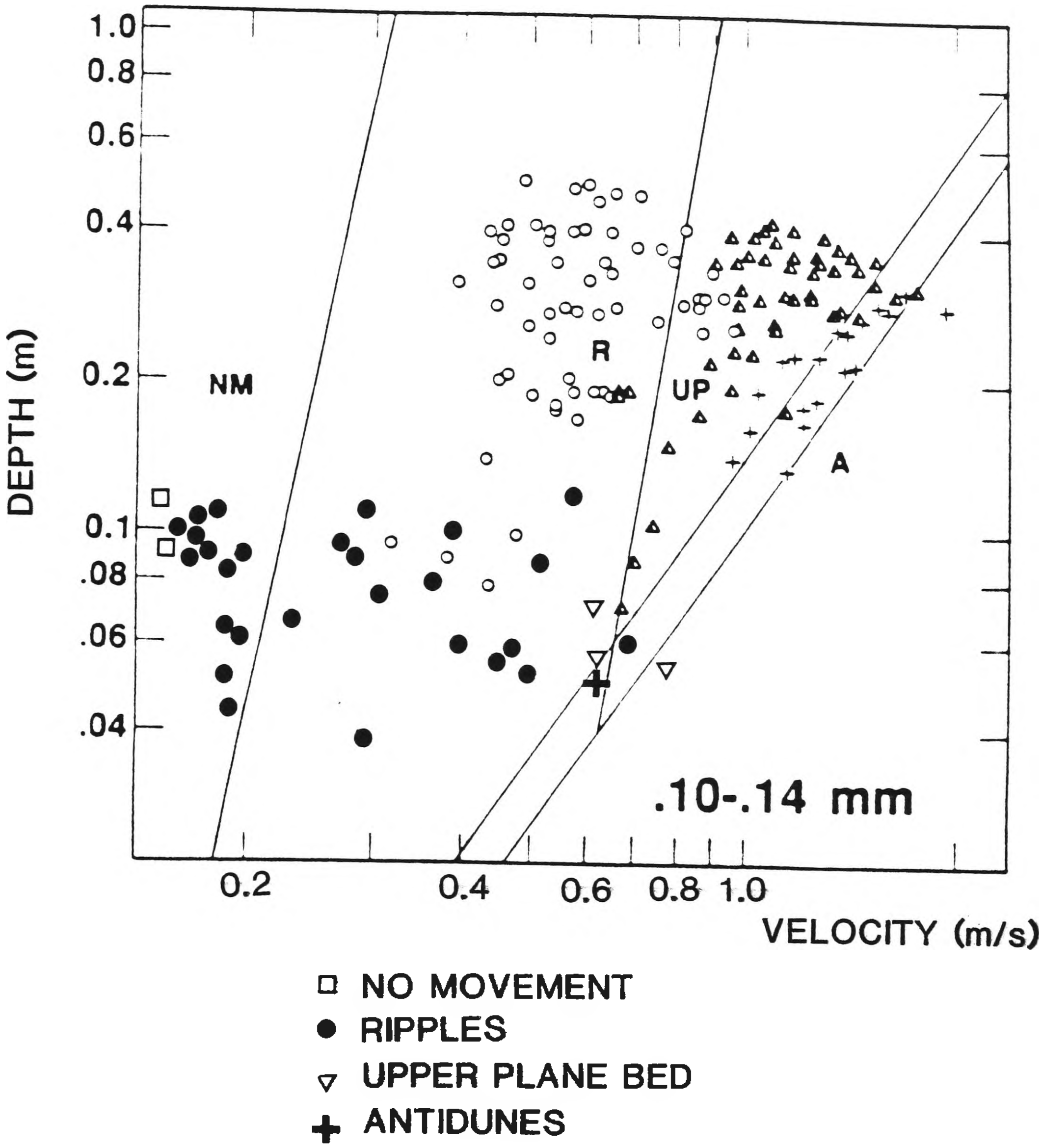


**FIGURE 4.4** Depth-velocity graph showing the various bed-phases, especially the NM and R bed states for a median sediment size range of 0.10-0.14 mm. NM=no movement; R=ripples; D=dunes; LP=lower regime plane bed; UP=upper-regime plane bed; A=antidunes. (Modified from Southard and Boguchwal, 1990).

Data for all 33 experimental flume runs were standardised to 10°C and plotted in Figure 4.4. All points representing upper flow regime and antidunes appear to agree with the bed phases shown. Of most interest is that points representing ripple bedforms plot in both the ripple (R) bed-phase **and** the no motion (NM) area of the diagram. This latter observation suggests that ripples can be generated at much lower flow velocities and therefore lower stream powers than for equivalent sized quartz grains.

Also the lower regime plane bed phases plot well away from the boundary between no motion and ripples. This again supports the view that the bedforms developed in this study occur at much lower velocities than would normally be expected. It is also interesting to note that the original data points given by Southard and Boguchwal (1990) do not extend below flow velocities of 0.35 $m.s^{-1}$. Yet velocities of <0.1 $m.s^{-1}$ were sufficient to generate small scale ripples in the flume.

It is clear from the diagram that the initiation of sediment transport for the aggregated sediment occurs at much lower flow velocities and flow depths than for equivalent sized quartz grains. This is primarily the result of the lower density of the aggregated sediment allowing it to be readily transported at much lower flow rates than for similar sized clastic sediment.

### 4.4.2 Suspended Load Measurements

Suspended sediment was sampled in 27 of the 33 experimental runs and these results were initially presented as sediment concentration ($g.l^{-1}$) (Table

4.2) and converted into a sediment transport rate ($kg.hr^{-1}$) and unit transport rate ($kg.\ hr^{-1}.m^{-2}$) (Table 4.5).

A plot of suspended sediment transport rates ($kg.hr^{-1}$) against flow velocity ($m.s^{-1}$) on a 5-cycle semi-log graph for six sediment batches is presented in Figure 4.5. Measured unit transport rates (Table 4.5) ranged between zero and nearly 129,884 $kg.hr^{-1}.m^{-2}$.

Applying a regression analysis to the complete data set in Figure 4.5, reveals no significant relationship between suspended sediment transport and flow velocity. In fact, this tends to be the case for most of the hydraulic parameters when regressed against suspended sediment transport. Closer examination of Figure 4.5, showed that the relationship within an individual sediment batch was much better defined than for the total data set. This is because with each change of sediment the clay aggregates start to break down at a rate dependent on the energy of the flow and the duration of the run. The results are more variable between runs than they are within the single run, so in the latter situation the sediment exhibits more uniform sediment characteristics (Table 4.6). Therefore, each sediment batch was examined independently.

### 4.4.3 Bedload Measurements

Bedload transport was recorded for 21 of the 33 flume runs and are presented below in Table 4.7 in two forms: gross transport rate ($kg.hr^{-1}$) and unit transport rate ($kg.hr^{-1}.m^{-1}$).

| Suspended Sediment Transport Rates | | |
|---|---|---|
| Run Number | Gross Transport Rate (kg.hr$^{-1}$) | Unit Transport Rate (kg.hr.$^{-1}$m$^{-2}$)* |
| 3 | 0.06 | 2.05 |
| 4 | 220.10 | 8151.85 |
| 5 | 0.35 | 7.94 |
| 6 | 0.45 | 9.52 |
| 7 | 0.44 | 9.31 |
| 8 | 11.25 | 233.64 |
| 9 | 39.90 | 886.67 |
| 11 | 0.17 | 3.85 |
| 12 | 0.47 | 10.77 |
| 13 | 0.92 | 21.52 |
| 14 | 32.79 | 877.91 |
| 15 | 6.33 | 251.19 |
| 18 | 20.19 | 954.61 |
| 19 | 34.51 | 1420.16 |
| 20 | 34.85 | 1408.08 |
| 21 | 89.77 | 3627.07 |
| 22 | 12.77 | 436.58 |
| 23 | 66.33 | 2267.69 |
| 24 | 148.61 | 4403.26 |
| 25 | 331.32 | 12479.10 |
| 26 | 718.36 | 27523.37 |
| 27 | 0.32 | 6.97 |
| 28 | 1.60 | 38.23 |
| 29 | 2.68 | 69.25 |
| 30 | 10.77 | 257.35 |
| 31 | 73.41 | 1896.90 |
| 32 | 73.46 | 2863.94 |
| 33 | 3916 | 129884 |

* Sediment transport rate per unit cross-sectional flow area (kg.hr$^{-1}$.m$^{-2}$)

**TABLE 4.5**

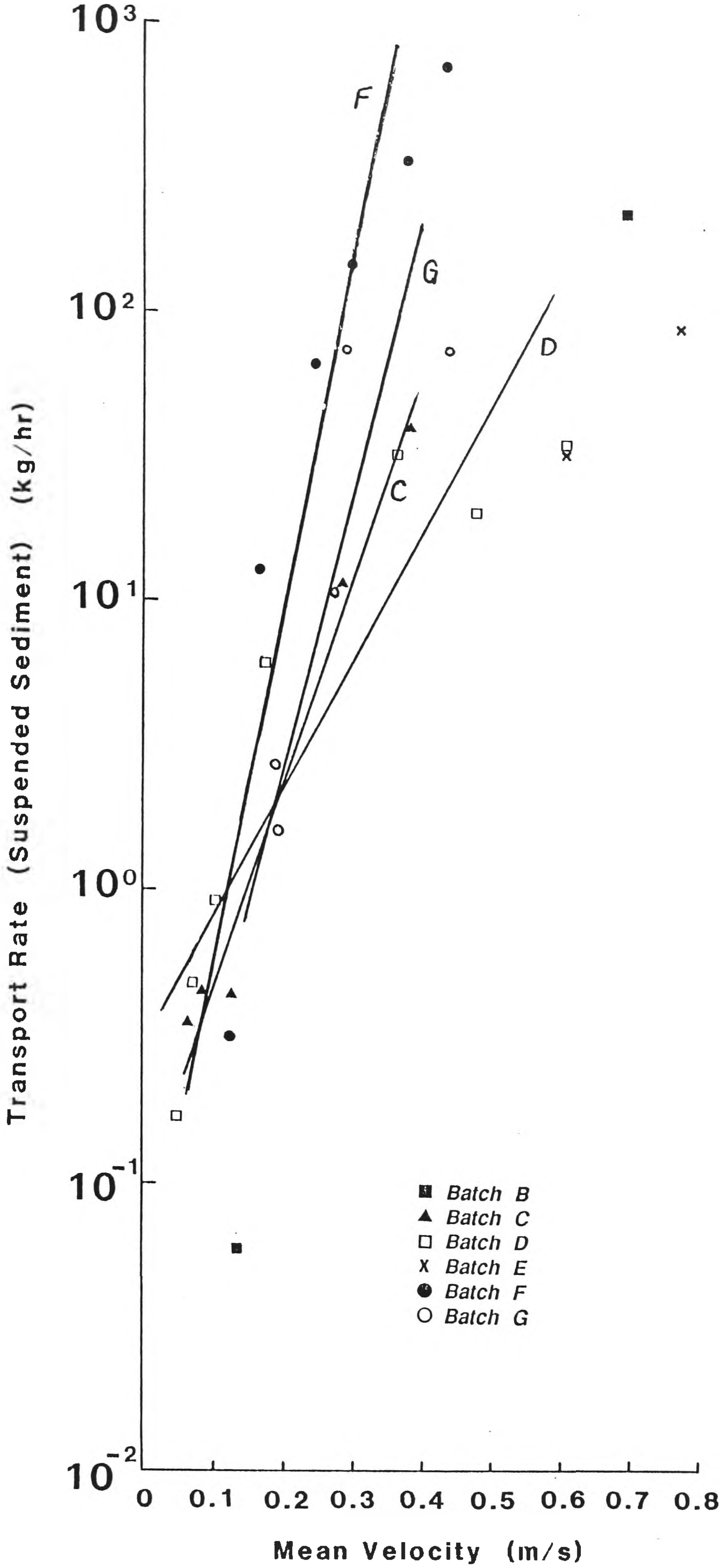


Figure 4.5 Suspended sediment transport rate (kg/hr) as a function of mean flow velocity (m/s) for each sediment batch.

| Statistical relationship between suspended sediment transport and hydraulic parameters for individual sediment batches. | | |
|---|---|---|
| **BATCH C Runs 5-10** | | |
| **Independent Variable: SUSPENDED LOAD n=5** | | |
| Dependent Variable | Regression Coefficient | Correlation Coefficient ($R^2$) |
| Velocity | 0.93 | 0.87 |
| Discharge | 0.91 | 0.83 |
| Slope | 0.95 | 0.89 |
| Friction Factor | -0.54 | 0.29 |
| Shear Stress | 0.95 | 0.90 |
| Stream Power | 0.97 | 0.95 |
| Reynold's Number | 0.92 | 0.84 |
| Froude Number | 0.94 | 0.89 |
| **BATCH D Runs 11-19** | | |
| **Independent Variable: SUSPENDED LOAD n=7** | | |
| Dependent Variable | Regression Coefficient (R) | Correlation Coefficient ($R^2$) |
| Velocity | 0.85 | 0.73 |
| Discharge | 0.92 | 0.84 |
| Slope | 0.63 | 0.40 |
| Friction Factor | -0.48 | 0.23 |
| Shear Stress | 0.63 | 0.40 |
| Stream Power | 0.74 | 0.54 |
| Reynold's Number | 0.92 | 0.85 |
| Froude Number | 0.86 | 0.74 |
| **BATCH F Runs 22-27** | | |
| **Independent Variable: SUSPENDED LOAD n=6** | | |
| Dependent Variable | Regression Coefficient (R) | Correlation Coefficient ($R^2$) |
| Velocity | 0.93 | 0.86 |
| Discharge | 0.85 | 0.73 |
| Slope | 0.84 | 0.70 |
| Friction factor | -0.54 | 0.29 |
| Shear Stress | 0.80 | 0.65 |
| Stream Power | 0.98 | 0.95 |
| Reynold's Number | 0.88 | 0.77 |
| Froude Number | 0.94 | 0.88 |

| BATCH G Runs 28-33 | | |
|---|---|---|
| **Independent Variable: SUSPENDED LOAD n=6** | | |
| Dependent Variable | Regression Coefficient (R) | Correlation Coefficient ($R^2$) |
| Velocity | 0.80 | 0.64 |
| Discharge | 0.65 | 0.42 |
| Slope | 0.60 | 0.36 |
| Friction Factor | -0.64 | 0.41 |
| Shear Stress | 0.49 | 0.24 |
| Stream Power | 0.64 | 0.41 |
| Reynold's Number | 0.76 | 0.57 |
| Froude Number | 0.78 | 0.60 |
| | | **TABLE 4.6** |

A wide range of bedload transport rates were recorded varying between zero and 277.1 $kg.hr^{-1}$(Table 4.7). When these transport rates were compared with other published figures from both field and flume settings (Brownlie, 1981), it becomes clear that those in this study are extremely high (see later discussion in Chapter 5).

As with suspended sediment transport, there is very little correlation between bedload transport and the flow variables when all the bedload data for all runs were grouped together (Figure 4.6). As a consequence, flow data for each sediment change was examined independently (Table 4.8) with much more success.

### 4.4.4 Relationships between sediment concentration and the flow variables.

As with clastic sediments, recognisable relationships exist between the transport rates obtained here (bedload and suspended load) and the flow parameters (velocity and unit stream-power). However, because of changes in aggregate size and suspended load concentration resulting from the comminution of mud aggregates during transport, these relationships are not stable through time. One cause of this is that fine suspended load produced from the breakdown of the aggregated sediment settles on the bed and increases the entrainment threshold for the remaining bedload aggregates.

| Bedload Transport Rates | | |
|---|---|---|
| **Run Number** | **Gross Transport Rate ($kg.hr^{-1}$)** | **Unit Transport Rate ($kg.hr^{-1}.m^{-1}$)*** |
| 7 | 0.11 | 0.24 |
| 8 | 0.38 | 0.84 |
| 9 | 1.56 | 3.47 |
| 13 | 0.28 | 0.62 |
| 14 | 3.32 | 7.38 |
| 15 | 5.37 | 11.93 |
| 16 | 2.28 | 5.07 |
| 17 | 1.79 | 3.98 |
| 18 | 2.28 | 5.07 |
| 19 | 61.57 | 136.82 |
| 20 | 74.54 | 165.64 |
| 21 | 127.55 | 283.44 |
| 22 | 10.40 | 23.11 |
| 23 | 30.80 | 68.44 |
| 24 | 81.80 | 181.77 |
| 25 | 172.20 | 382.67 |
| 26 | 198.00 | 440.00 |
| 28 | 0.70 | 1.56 |
| 29 | 1.50 | 3.33 |
| 30 | 10.50 | 23.33 |
| 31 | 15.40 | 34.22 |
| 32 | 177.10 | 393.56 |
| 33 | 277.15 | 615.78 |

* Sediment transport rate per unit channel width ($kg.hr^{-1}.m^{-1}$)

**TABLE 4.7**

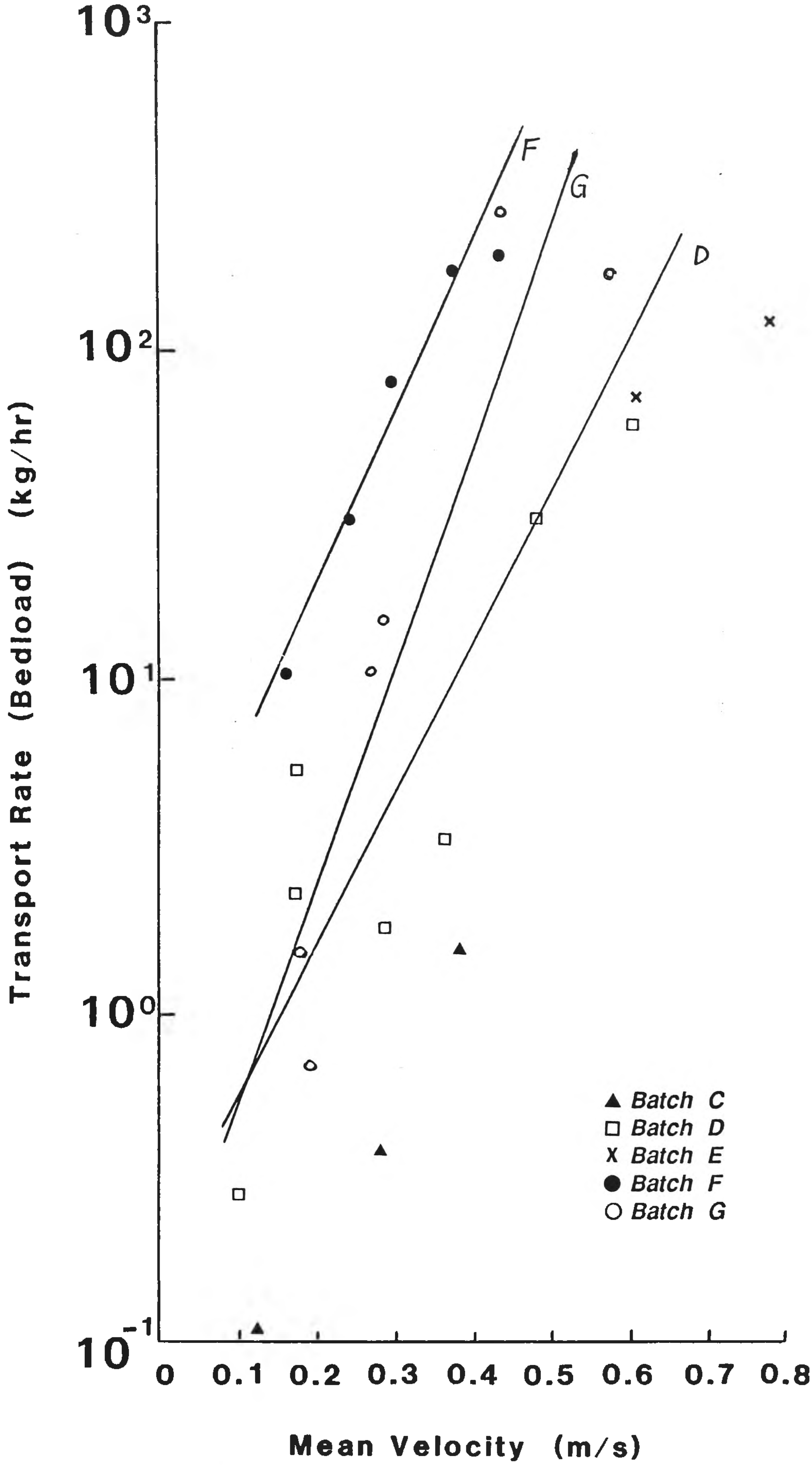


Figure 4.6 Bedload transport rate (kg/hr) as a function of mean flow velocity (m/s) for each sediment batch.

| Statistical relationship between bedload transport and hydraulic parameters for individual sediment batches. | | |
|---|---|---|
| **BATCH D Runs 11-19** | | |
| **Independent Variable: BEDLOAD n=7** | | |
| Dependent Variable | Regression Coefficient (R) | Correlation Coefficient ($R^2$) |
| Velocity | 0.84 | 0.70 |
| Discharge | 0.60 | 0.36 |
| Slope | 0.87 | 0.76 |
| Friction Factor | -0.21 | 0.04 |
| Shear Stress | 0.87 | 0.76 |
| Stream Power | 0.91 | 0.83 |
| Reynold's Number | 0.68 | 0.46 |
| Froude Number | 0.87 | 0.75 |
| **BATCH F Runs 22-27** | | |
| **Independent Variable: BEDLOAD n=5** | | |
| Dependent Variable | Regression Coefficient (R) | Correlation Coefficient ($R^2$) |
| Velocity | 0.96 | 0.93 |
| Discharge | 0.64 | 0.48 |
| Slope | 0.60 | 0.36 |
| Friction Factor | -0.74 | 0.54 |
| Shear Stress | 0.54 | 0.29 |
| Stream Power | 0.82 | 0.67 |
| Reynold's Number | 0.90 | 0.81 |
| Froude Number | 0.97 | 0.95 |
| **BATCH G Runs 28-33** | | |
| **Independent Variable: BEDLOAD n=6** | | |
| Dependent Variable | Regression Coefficient (R) | Correlation Coefficient ($R^2$) |
| Velocity | 0.68 | 0.46 |
| Discharge | 0.38 | 0.14 |
| Slope | 0.74 | 0.55 |
| Friction factor | -0.39 | 0.15 |
| Shear Stress | 0.58 | 0.34 |
| Stream Power | 0.56 | 0.31 |
| Reynold's Number | 0.47 | 0.22 |
| Froude Number | 0.76 | 0.58 |

**TABLE 4.8**

### 4.5 Role of salt (NaCl) in the development of the aggregated sediment.

Salt concentrations of the aggregated sediment were measured between 150 and 200 ppm or <0.02% of the sample (Table 4.1). This suggests that salt is **not** an important ingredient in the development of the clay pellets on the Cooper floodplain. Their formation has been attributed by Nanson et al. (1986, 1988) and Rust and Nanson (1989) to the presence of expandable clays. As shown here, aggregates can be formed from disaggregated alluvium after only two to three wetting-drying cycles, providing clear evidence that the aggregates can be developed *in situ* on the floodplains and under non-saline conditions. Aggregates appear to be formed at the floodplain surface as a result of flooding and rainstorms. Puddling of the soil followed by drying in intense sunlight and hot winds produces a light "fluffy" structure with a very high void ratio. The surface soil exhibits very well developed aggregates that are easily entrained by floodwaters and are subject to rill erosion during heavy rainstorms. As more alluvial mud accumulates at the surface, the subsoil becomes compacted, increasingly so with depth and the pelleted structure disappears (Nanson et al., 1988). At a depth of about 1-2 m the original pelleted aggregates are compressed into a uniform clay matrix with grains of quartz sand (Plate 4.5).

With the hot daytime and summer temperatures in this region these alluvial soils develop deep, wide cracks characteristic of a Vertisol, and these assist in the self-mulching process. Loose soil falls down the cracks and is compressed when the soil is wetted by rainfall or flooding. As the clay expands, the soil heaves at the surface forming mounds. With drying the soil

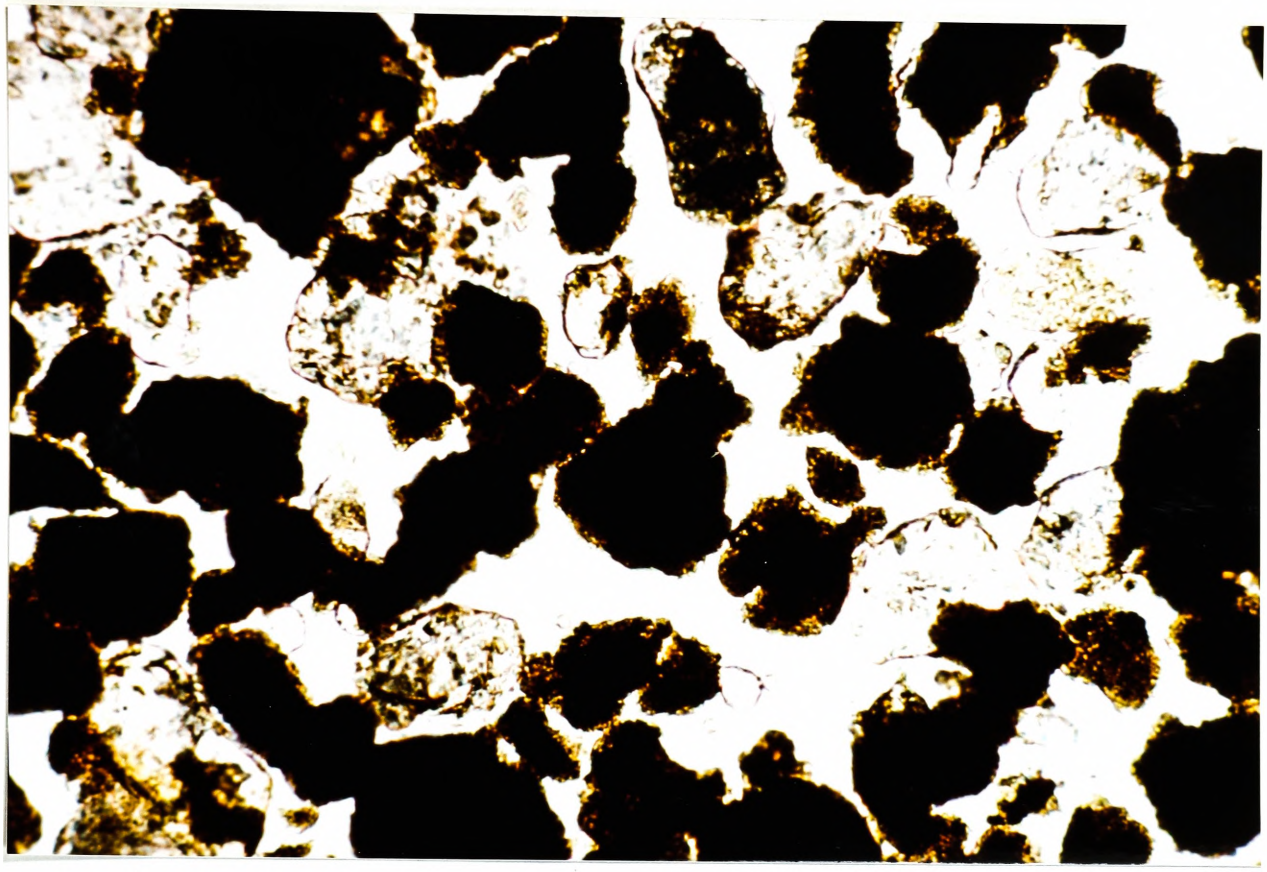

Plate 4.5 (a)

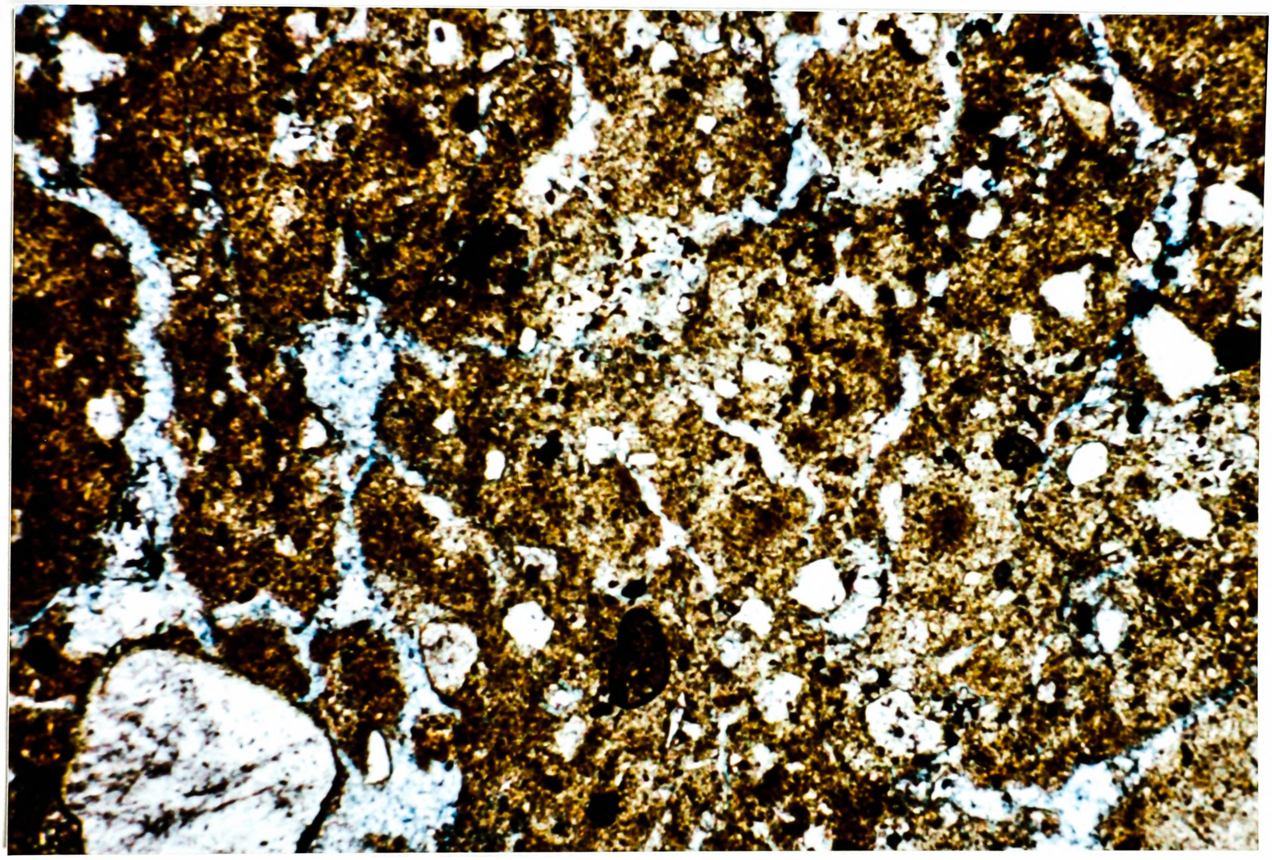

Plate 4.5 (b)

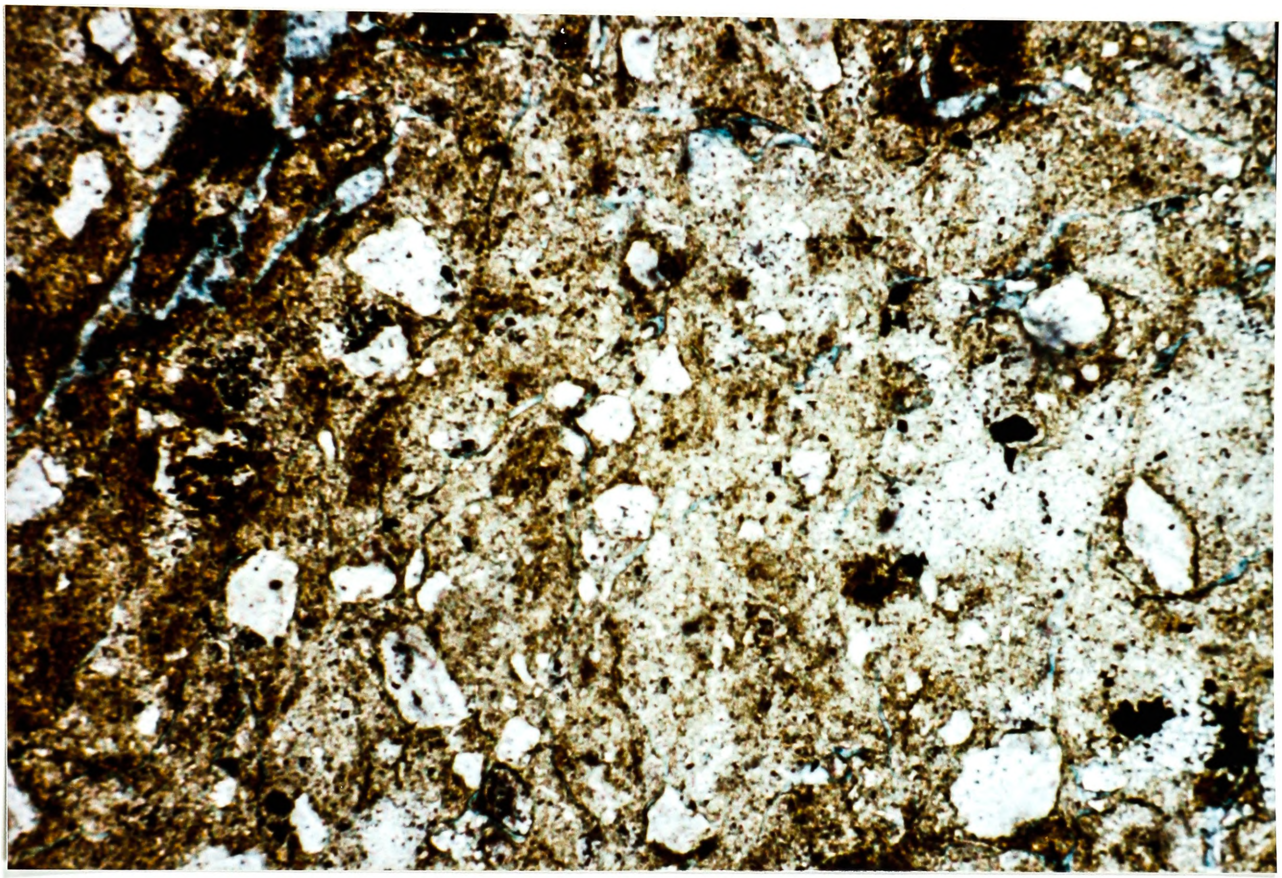

Plate 4.5 (c)

Plate 4.5 Floodplain sediment from Naccowlah in various stages of compaction resulting from floodplain accretion.

(a) Loose surface mud showing pellets (black) and quartz sand grains (opaque). HFV (Horizontal field of view) = 1.6 mm.
(b) Thin section from 1 m beneath floodplain surface. HFV = 1.2 mm.
(c) Thin section at 2 m depth. HFV = 1.2 mm.

With depth the mud compacts to an almost structureless matrix around the quartz grains.

shrinks and the cracks reform. By this process, the soil is "stirred" or self-mulched, and mixed within a zone of mixing of about 0.5 m from the surface.

Preservation and maintenance of the soil aggregates is undoubtedly more effective in the field than in the highly turbulent laboratory flume. In a flood event, because they are water stable, the aggregates may be transported many hundreds of metres or even several kilometres before being deposited. Furthermore, because they are not completely broken down by transport, clay pellets in the field probably require only one wetting-drying cycle before being available for transport. The result is an abundance of aggregated sediment available for transport, some formed *in situ* from disaggregated sediment but most transported intact from upstream localities.

## 4.6 Conclusion

In summary, the sediment was found to contain >60% clay in fine sand-sized pedogenic aggregates ($d_{50}$=0.10 mm) with densities lower than equivalent sized quartz grains (2300 $kg.m^{-3}$ compared with 2660 $kg.m^{-3}$). Low solute concentrations (<0.02%) suggest that salt plays **no** role in the development of these aggregates. As well, completely disaggregated alluvium was regenerated into aggregated sediment after 2-3 wetting/drying cycles. Partially disaggregated sediment in the field would probably only require one cycle to reform transportable aggregates.

Bedforms developed in the flume using the aggregated sediment ranged from lower regime plane beds and ripples, through to upper regime plane beds and antidunes. There is general agreement between published bedform existence diagrams for 0.10 mm sand sizes and the experimental data for mud aggregates presented here except that all the bedform types form from mud pellets more readily at lower stream powers than do their equivalents in quartz sand. This is due to the significantly lower densities of the mud aggregates.

Measured peak bedload concentrations were high in comparison with other flume studies in the literature (Brownlie, 1981) and were attributed to the lower aggregate density of the sediment. Strong correlations were found between bed and suspended load and most of the flow variables.

# CHAPTER 5 DISCUSSION AND CONCLUSION

## 5.1 Properties of the floodplain sediment and their effect on sediment transport.

The aggregated alluvial sediments from Cooper Creek exhibit some unique characteristics. Although formed of more than 60% clay they are shown to have an aggregate mean diameter of 0.1 mm which is equivalent to fine sand. Due consideration of the way in which the sediment is wetted in the field was important as this effects the aggregate diameter (Table 4.1). Immersion wetting results in an aggregate size nearly an order of magnitude less than that resulting from tension wetting, but is the most appropriate size for fluvial interpretations. Large-scale overbank flooding results in immersion wetting of surface sediments over the floodplains of Cooper Creek immediately prior to their entrainment as bedload.

An aggregate density of 2300 $kg.m^{-3}$ is significantly less than that for quartz sand (2660 $kg.m^{-3}$) and has important implications for sediment transport. The aggregates can be entrained at much lower stream powers and shear stresses than equivalent size quartz grains and are maintained in the flow for long periods of time. The lower entrainment threshold of this sediment is clearly evident in Figure 4.4. Visual observations through the sides of the flume show that the aggregated sediment moves as rolling and sometimes saltating bedload, in much the same way as quartz sand.

In the flume experiment the aggregates were found to be extremely water stable. In some cases the flume was operated continuously for 24 hours before significant disaggregation of the clay aggregates occurred, an observation also made by Nanson et al., (1986) in a similar flume experiment. Due to turbulence in the return pipe and impeller of the pump, the amount of disaggregation that occurred in the flume would be much higher than would occur in natural field conditions. Although in field situations the sediment would be subjected to long periods of inundation due to slow moving flood waters typical of the low gradient interior drainage network of Central Australia, most of the active transport would occur during passage of the leading edge of the floodwave (Nanson et al., 1986) and, therefore, could be over in a matter of hours or a few days. It is envisaged that the sediment may through time disaggregate due to prolonged wetting but the rate of disaggragation is probably very much lower than in the highly turbulent flume.

Bedload transport of aggregates was the dominant mode of sediment transport at high flow rates while suspended-load transport dominates at lower flow rates (Table 4.2, 4.5, 4.7; Figure 4.5, 4.6). Given the low entrainment threshold of the aggregated sediment, it is not surprising that transport rates are very high. Compared with a compilation of flume and river data over the last 100 years (Brownlie, 1981), peak bed and suspended material concentrations presented in this study are significantly higher (Table 4.5, 4.7). Suspended load transport rates ranged between zero and 129,884 $kg.hr^{-1}.m^{-2}$, zero and 615.8 $kg.hr^{-1}.m^{-1}$ for bedload. Considering these transport rates, the width of the flood channel (about 16 km at Durham Downs and >50 km south of Windorah (Figure 1.1), a floodplain surface which has a low entrainment threshold, and the duration of some floods (large floods can take several weeks to pass because of the very low gradients), the volumes of sediment in transport during a single flood must be vast. The movement of sediment must be enormous during the early stages of an individual flood when the dry sediment is first inundated and then entrained by the floodwaters at the leading edge of the floodwave.

However, due to the arid nature of the area, the very low gradients and the relatively infrequent nature of flood events, the total sediment yield per decade or century may be relatively small.

## 5.2 Development of bedforms

The aggregated sediment of the Cooper floodplain are readily transported as rolling bedload of fine-sand size and are water stable, it is not surprising that bedforms do develop. While there is little detailed data on bedforms for sediments with median diameters less than 0.2 mm, the information obtained here for the transport and deposition of aggregates with a median size of 0.1 mm indicates that they have very different transport and depositional properties to clastic sands that are only slightly coarser (Figure 4.3). Each bedform type formed of aggregates occurred at lower stream powers than is the case for quartz sand only (Simons et al., 1965) and it is clear that incipient motion occurs at extremely low stream powers and shear stresses (Figure 4.3, 4.4). With increasing stream power, the progression of bedforms was as follows: plane bed (no motion), ripples, plane bed (upper-regime) and antidunes (Figure 4.3).

The identification of bedform development in non-saline muddy sediments has important geological implications. Sedimentologists have in the past attributed bedform structures in mudrock sequences to saline depositional environments on oceanic continental margins where turbidity currents prevail (Allen, 1968; 1985a,b) and in arid areas where extensive halite deposits are present (Karcz and Zak, 1987). In this study, an aggregated clay-rich sediment developed bedforms under conditions similar to those that generate bedforms from quartz grains of similar size.

To date, only Rust and Nanson (1989) have proposed fluvial transport conditions similar to those described here to explain ancient mud units in the stratigraphic record.

## 5.3 Channel planform development.

The observations by Nanson et al. (1986) of the coexistence of two distinct yet contemporary channel planforms (braided and anastomosing) and the presence of braided channels formed in mud are especially noteworthy. The phenomenon of mud braids they attributed to the transport of clay-rich sediment as fine sand-sized pedogenic aggregates with densities lower than quartz grains.

Braid channels normally require relatively steep channel gradients to form (Schumm, 1981), however, the abundant light-weight mud aggregates in the Channel Country result in braids forming at slopes of about 0.0002

(Nanson et al., 1986). During low to moderate (in-channel) flows, water and sediment are transported in the numerous anastomosing channels. In these channels, gradients can be very low (<0.0002). At high flows, floodwaters overtop the floodplain and take a more direct course downstream developing a slightly steeper braided channel system in the loose friable aggregated sediments over the floodplain surface. The relatively low density of the sediment aggregates means that large quantities of this material can be entrained as bedload at relatively low stream powers.

## 5.4 Conclusion.

This study has examined the fluvial transport of aggregated clay-rich soil in a laboratory flume. The aggregates of median diameter 0.10 mm behave in an analogous manner to fine sand in that they develop lower, transitional and upper regime bedforms in response to varying stream power.

At higher flow rates, most of the sediment was transported as bedload at rates that were shown to be very high when compared to those for quartz sand (Brownlie, 1981). Suspended load transport dominated at lower flow rates. The high rates of transport are attributed to the more mobile nature of the aggregates with lower densities and therefore lower entrainment thresholds than equivalent sized quartz grains.

Aggregate formation is believed to be largely a function of the clay mineralogy of the sediment, especially the presence of the expandable clays such as smectite (Rust and Nanson, 1989). The importance of salt (NaCl) in the formation of these aggregates was insignificant. The aggregates were shown to form in the laboratory after only two to three wetting-drying cycles.

Given the clay-rich nature of sediment in Cooper Creek the presence of anastomosing channels is to be expected, however, the coexistence of both anastomosing and braided channels is not (Nanson et al., 1986). Braids are normally present where sediment load is coarse, slopes are steep and flow depths are shallow (Leopold and Wolman, 1957). The braid features in Cooper Creek can be attributed to: a) steeper channel gradients produced by downvalley flow over the floodplains during the passage of a flood; b) the highly mobile nature of the sediment with low entrainment thresholds aided by the low density of the sediment and its highly dispersed fluffy nature when dry; c) the ability of the sediment to be transported as bedload aggregates; and d) the durability of the sediment aggregates during prolonged periods of flow.

# REFERENCES


Alberts, E.E., Wendt, R.C. and Piest, R.F. (1983) Physical and chemical properties of eroded soil aggregates. Trans. A.S.C.E., 26, 465-471.

Allen, J.R.L. (1968) Current Ripples: Their relation to Patterns of water and sediment motion. North Holland Publ. Co., Amsterdam, 433pp.

Allen, J.R.L. (1985a) Principles of Physical Sedimentology. George Allen and Unwin Ltd., London, 272pp.

Allen, J.R.L. (1985b) Loose-boundary hydraulics and fluid mechanics: selected advances since 1961 in Brenchley, P.J. and Williams, B.P.J., (ed.), Sedimentology: recent developments and applied aspects. Geol. Soc. Spec. Publ., No. 18, 7-28.

American Society of Civil Engineers, Task Force on Bedforms in Alluvial Channels. (1966) Nomenclature for bedforms in alluvial channels, Am. Soc. Civil Engineers Proc., Jour. Hyd. Div., v.92, No.3, 51-64.

American Society of Civil Engineers, Task Force on Bedforms in Alluvial Channels. (1968) Discussion of "Nomenclature for bedforms in alluvial channels" by Task Force on Bedforms in Alluvial Channels of the Committee on Sedimentation, A.S.C.E., Proc., Jour. Hyd. Div., v.94, No.5, 1333-1335.

Ashley, G.M. (1990) Classification of large-scale subaqueous bedforms: A new look at an old problem. J. Sed. Petrol., 60, 160-172.

Aziz, N.M. and Scott, D.E. (1989) Experiments on sediment transport in shallow flows in high gradient channels. Hydrol. Sci. J., 34, 465-478.

Bagnold, R.A. (1956) The flow of cohesionless grains in fluids. Phil. Trans. Roy. Soc. London, Ser. A., 249, 234-297.

Brownlie, W.R. (1981) Compilation of alluvial channel data. Laboratory and Field. Rept. KH-R-43B, California Institute of Technology, Pasadena, 209pp.

Boguchwal, L.A. and Southard, J.B. (1990) Bed configurations in steady unidirectional water flows. Part 1. Scale model study using fine sands. J. Sed. Petrol., 60, 649-657.

Bouyoucous, G.J. (1928) The hydrometer method for making a very detailed mechanical analysis for soils. Soil Sci., v. 26, 233.

Bowler, J.M. (1973) Clay Dunes: Their occurrence, formation and environmental significance. Earth Sci. Rev., 9, 315-338.

Boyland, D.E. (1974) Vegetation, in Western Arid Region - Land Use Study - Part 1, Tech. Bull., 12, Division of Land Utilisation, D.P.I., Brisbane, Queensland, 47-70.

Butler, B.E. (1956) Parna - an aeolian clay. Aust. J. Sci., 18, 145-151.

Butler, B.E. (1974) A contribution towards the better specification of parna and some other aeolian clays in Australia. Zeitschrift fur Geomorphologie, 20, 106-116.

Cheel, R.J. (1990) Horizontal lamination and the sequence of bed phases and stratification under upper-flow-regime conditions. Sedimentol., 37, 517-530.

Coughlan, K.J. (1984) The structure of Vertisols, in McGarity, J., Hault, P. and So. K., (ed.), The Properties and Utilisation of Cracking Clay Soils, Reviews in Rural Science, No. 5, Uni. of New England, 87-96.

Dalrymple, R.W., Knight, R.J. and Lambiase, J.J. (1978) Bedforms and their hydraulic stability relationships in a tidal environment, Bay of Fundy, Canada. Nature, 275, 100-104.

Dare-Edwards, A.J. (1982) Clay pellets of clay dunes: types, mineralogy, origin and effect of pedogenesis, in Wasson, R.J. (ed.) Quaternary Dust Mantles of China, New Zealand and Australia, Aust. Nat. Univ., 179-189.

Dawson, N.M. (1974) Geology and Landform, in Western Arid Region - Land Use Study - Part 1, Tech. Bull., 12, Division of Land Utilisation, D.P.I., Brisbane, Queensland, 12-17.

Dawson, N.M. and Ahern, C.R. (1974) Soils, in Western Arid Region - Land

Use Study - Part 1, Tech. Bull., 12, Division of Land Utilisation, D.P.I., Brisbane, Queensland, 12-17.

Day, P.R. (1965) Particle Fractionation and Particle-Size Analysis, in Black, C.A. (ed.) Methods of Soil Analysis, Part 1, Am. Soc. Agronomy, No. 9, Madison, Wisconsin, 545-577.

Engelund, F. (1966) Hydraulic resistance of alluvial streams. Jnl. Hyd. Div., A.S.C.E., v. 92, No. 2, 315-326.

Folk, R.L. (1968) Petrology of Sedimentary Rocks. Hemphills, Austin, Texas, 170pp.

Fleming, B.W. (1988) Zur Klassifikation subaquatischer, stromungstrans versaler Transportkorper. Boch. geol. u. geotechn. Arb., 29, 44-47.

Gabriels, D. and Moldenhauer, W.C. (1978) Size distribution of eroded material from simulated rainfall: effect over a range of soil texture. Soil Sci. Soc. Am. J., 42, 954-958.

Gilbert, G.K. (1914) The transportation of debris by running water. U.S.G.S., Prof. Paper, 86.

Gilley, J.E., Finkner, S.C., Spomer, R.G. and Mielke, L.N. (1986) Size distribution of sediment as affected by corn residue. Trans. A.S.A.E., 29, 1273-1277.

Graf, W. (1971) Hydraulics of Sediment Transport, McGraw-Hill Book Co., Inc., New York, N.Y.

Guy, H.P., Simons, D.B. and Richardson, E.V. (1966) Summary of alluvial channel data from flume experiments, 1956-61. U.S.G.S., Prof. Paper, 462-I, 96pp.

Harms, J.C., Southard, J.B., Spearing, D.R. and Walker, R.G. (1975) Depositional environments as interpreted from sedimentary structures and stratification sequences, Soc. Econ. Paleontologists and Mineralogists, Short Course 2, Dallas,161pp.

Harms, J.C., Southard, J.B. and Walker, R.G. (1982) Structure and sequence in clastic rocks. Soc. Econ. Paleontologists and Mineralogists, Short Course 9, Dallas, 250pp.

Jopling, A.V. and Forbes, D.L. (1979) Flume study of silt transportation and deposition. Geogr. Ann., 61, 67-85.

Karcz, I. and Zak, I. (1987) Bedforms in salt deposits of the Dead Sea brines. J. Sed. Pet, v. 57, No. 4, 723-735.

Kennedy, J.F. (1963) The mechanics of dunes and antidunes in erodible-bed channels. J. Fluid Mech., 16, 521-544.

Leopold, L.B. and Wolman, M.G. (1957) River channel patterns-braided, meandering and straight, U.S.G.S. Prof. Paper, 282B.

Loch, R.J. and Donnollan, T.E. (1983a) Field rainfall simulator studies on two clay soils of the Darling Downs, Queensland. I. The effects of plot length and tillage orientation on erosion processes and runoff and erosion rates. Aust. J. Soil Res., 21, 33-46.

Loch, R.J. and Donnollan, T.E. (1983b) Field rainfall simulator studies on two clay soils of the Darling Downs, Queensland. II. Aggregate breakdown, sediment properties and soil erodibility. Aust. J. Soil Res., 21, 47-58.

Loch, R.J. and Donnollan, T.E. (1989) Rill erosion of a self-mulching black earth. I. Effects of tillage treatment. Aust. J. Soil Res., 27, 525-534.

Loch, R.J., Maroulis, J.C. and Silburn, D.M. (1989) Rill erosion of a self-mulching black earth. II. Comparison of sediment transport equations. Aust. J. Soil Res., 27, 535-542.

Long, D.C. (1964) The size and density of aggregates in eroded material. M.Sc. Thesis, Iowa State Uni., Ames, Ia.

Lovell, C.J. and Rose, C.W. (1988) Measurement of soil aggregate settling velocities. I. A modified bottom withdrawal tube method. Aust. J. Soil Res., 26, 55-71.

Lu, J.Y., Cassol, E.A., Foster, G.R. and Neibling, W.H. (1988) Selective transport and deposition of sediment particles in shallow flow. Trans. A.S.A.E., 31, 1141-1147.

Mantz, P.A. (1978) Bedforms produced by fine, cohesionless, granular and flakey sediments under subcritical water flows. Sedimentol., 25, 83-103.

Maroulis, J.C., Loch, R.J., Foley, J. and Silburn, D.M. (in press) Erosion processes on a cracking clay soil. Relative importance of rilling on 22.5 m long rainulator plots. Earth Surf. Proc.

Middleton, G.V. and Southard, J.B. (1978) Mechanics of sediment movement. S.E.P.M. Short Course No. 3, Tulsa, 246pp.

Mitchell, J.K., Mostaghimi, S. and Pond, M.C. (1983) Primary particle and aggregate size distribution of eroded soil from sequenced rainfall events. Trans. A.S.A.E., 26, 1773-1777.

Nanson, G.C., Rust, B.R. and Taylor, G. (1986) Coexistent mud braids and anastomosing channels in an arid zone river: Cooper Creek, Central Australia. Geology, 14, 175-178.

Nanson, G.C., Young, R.W., Price, D.M. and Rust, B.R. (1988) Stratigraphy, Sedimentology and Late Quaternary Chronology of the Channel Country of Western Queensland, in Warner, R.F. (ed.) Fluvial Geomorphology of Australia, Sydney, N.S.W., 151-175.

Nimmo, W.H.R. (1947) Summary of the hydrology of Cooper's Creek. Bureau of Investigations, Tech. Bull., No. 1, 134-148.

Northcote, K.H. (1965) A factual key for the recognition of Australian soils. 2nd Edn., C.S.I.R.O., Aust. Div. Soils, Divl. Rept., 2/65.

Ogilvie, C. (1947) The hydrology of Cooper's Creek. Bureau of Investigations, Tech. Bull., No. 1, 36-70.

Parthenides, E. (1965) Erosion and deposition of cohesive soils, J. Hyd. Div., A.S.C.E., 91, 105-139.

Rathbun, R.E. and Guy, H.P. (1967) Measurement of hydraulic and sediment transport variables in a small recirculating flume. Water Resour. Res., 3, 107-122.

Reineck, H-E. and Singh, I.B. (1980) Depositional Sedimentary Environments. 2nd End., Springer-Verlag, Berlin.

Rees, A.I. (1966) Some flume experiments with a fine silt. Sedimentol., 6, 209-240.

Richards, K.J. (1980) The formation of ripples and dunes on an erodible bed. J. Fluid Mech., 99, 597-618.

Richards, L.A. (1954) (ed.). Diagnosis and improvement of Saline and Alkali soils. U.S.D.A., Agr. Handbook, No. 60.

Rust, B.R. (1981) Sedimentation in an arid-zone anastomosing fluvial system: Cooper Creek, Central Australia. J. Sed. Petrol., 52, 745-755.

Rust, B.R. and Nanson, G.C. (1986) Contemporary and paleochannel patterns and the Late Quaternary stratigraphy of Cooper Creek, Southwest Queensland, Australia. Earth Surf. Proc. and Landforms, 11, 581-590.

Rust, B.R. and Nanson, G.C. (1989) Bedload transport of mud as pedogenic aggregates in modern and ancient rivers. Sedimentol., 36, 291-306.

Schumm, S.A. (1981) Evolution and the response of the fluvial system, sedimentological implications, Soc. Econ. Paleontologists and Mineralogists Spec. Pub., 31, 19-29.

Simons, D.B. and Richardson, E.V. (1966) Resistance to flow in alluvial channels. U.S.G.S., Prof. Paper, 422-J.

Simons, D.B., Richardson, E.V. and Nordin, C.F., Jr. (1965) Sedimentary structures generated by flow in alluvial channels, Soc. Econ. Paleontologists and Mineralogists Spec. Pub., 12, 34-52.

Smith, G.D. (1984) Soil constituent and prehistory effects on aggregate porosity in cracking clays, in McGarity, J., Hault, P. and So. K., (ed.), The Properties and Utilisation of Cracking Clay Soils, Reviews in Rural Science, No. 5, Uni. of New England, 87-96.

Southard, J.B. (1971) Representation of bed configurations in depth-velocity-size diagrams. J. Sediment Petrol., 41, 903-915.

Southard, J.B. and Harms, J.C. (1972) Sequence of bedform and stratification in silts, based on flume experiments. Am. Assoc. Petroleum Geol. Bull., 56, 654-655 (abstract).

Southard, J.B. and Boguchwal, L.A. (1990) Bed configurations in steady unidirectional water flows. Part 2. Synthesis of flume data. J. Sed. Petrol., 60, 658-679.

Stace, H.C.T., Hubble, G.D., Brewer, R., Northcote, K.H., Sleeman, J.R., Mulcahy, M.J. and Hallsworth, E.G. (1968) A Handbook of Australian Soils, Glenside, S.A., C.S.I.R.O.

Stanley, K.O. (1974) Morphology and hydraulic significance of climbing ripples with superimposed micro-ripple-drift cross- lamination in Lower Quaternary lake silts, Nebraska. J. Sediment. Petrol., 44, 472-483.

Swanson, N.P. and Dedrick, A.R. (1965) Soil particles and aggregates transported in runoff from simulated rainfall. Trans. A.S.A.E., 8, 437-440.

Twidale, C.R. (1972) Landform development in the Lake Eyre region, Australia. The Geographical Review, 62, 40-70.

Vanoni, V.A. and Brooks, N.H. (1957) Laboratory studies of the roughness and suspended load of alluvial streams. Rept. E-68,Sedimentation Laboratory, California Inst. Technology, Pasadena, 121pp.

Weakly, H.E. (1962) Aggregation of soil carried in runoff from simulated rainfall. Soil Sci. Soc. Am. Proc., 26, 511-512.

Whitehouse, F.W. (1947) The geology of the channel country of south-western Queensland. Bureau of Investigations, Tech. Bull. No. 1, 134-148.

Williams, G.E. (1970) Piedmont sedimentation and late Quaternary chronology in the Biskra region of the northern Sahara. Zeitschrift fur Geomorphologie, 10, 40-63.

Williams, G.P. (1971) Aids in designing laboratory flumes. U.S.G.S., Water Res. Div., Open-file Report, Washington, D.C.

Yalin, M.S. (1972) Mechanics of Sediment Transport. Pergamon Press, Oxford, 290pp.